

Morphology Control and Ordering of PS- b-PMMA Block Copolymer by The Use of Neutral Monolayer and E-beam Lithography

by

Babak Baradaran Shokouhi

A thesis
presented to the University of Waterloo
in fulfillment of the
thesis requirement for the degree of
Master of Applied Science
in
Electrical and Computer Engineering (Nanotechnology)

Waterloo, Ontario, Canada, 2015

AUTHOR'S DECLARATION

I hereby declare that I am the sole author of this thesis. This is a true copy of the thesis, including any required final revisions, as accepted by my examiners.
I understand that my thesis may be made electronically available to the public.

Abstract

As the conventional nanofabrication methods are reaching their limits of miniaturization, new methods are being studied to overcome this miniaturization challenge. Among the new emerging nanofabrication methods, bottom-up self assembly of Block Copolymers (BCPs) is gaining significant popularity among the researchers and the semiconductor industries. BCP self assembly has many advantages among which, low processing cost, high resolution, and large scale processing are the more prominent ones. Controlling the polymer fraction in the BCP mix leads to variety of different morphologies, these morphologies can be used to create nanofabrication masks and templates. A great amount of research has been conducted on how to control BCP morphologies. However, orientation of these BCP morphologies are very important and crucial to the nanofabrication technologies. Ideally, morphologies with perpendicular orientation to the surface of the substrate with very high aspect ratios are preferred for pattern transfer. To obtain this unique orientation many different methods have been studied, however in this research we employed a unique method to modify the surface energy of the substrate and create perpendicular morphologies for the BCP of PS-b-PMMA. Further, electron beam lithography was used to modify the properties of the PS-b-PMMA block copolymer in order to obtain different morphologies within the same BCP thin film.

Acknowledgements

I wish to express my sincere appreciation and gratefulness to my advisor Professor Bo Cui for his knowledge, insight, valuable guidance, and continuous encouragement throughout this research. He is always there when I need help. His advices always helped me not just in my thesis but in all aspects of my life. Indeed, my gratitude to him cannot be expressed in a few words and it is my honor to be his student.

I am also grateful to the members of my MASc. committee, Professor Mustafa Yavuz, Professor Guoxing Miao for their time and effort to improve the quality of this thesis. I am thankful to all members of the Waterloo Nanofabrication Group research group not only for their invaluable technical assistance but also for creating a warm, friendly, and welcoming environment.

I am indebted to many wonderful friends who have supported me even in the cold rainy days of my master studies. They have been always there to lend me a helping hand and made my time at Waterloo an enjoyable experience full of unforgettable memories. I would also like to recognize my colleagues Alireza Tari, Dr. Jian Zhang, Dr. Xiangcheng (Mike) Sun. I would also like to thank my group mates, who made our office enjoyable for this time.

Extended thank you goes to my Mother and Father for their support and patience during my education life. They taught me how to start with A,B,C and finish with a graduate degree. I will never forget their endless support and kindness and I cannot be thankful enough for their sacrifices. I am thankful to my caring brother, Arash Baradaran Shokouhi, he always ignites hope in me whenever I feel hopeless.

Dedication

To my most loving, caring and patient mother, Soheila Motamedi

To my always supporting father, Nasser Baradaran Shokouhi

Table of Contents

AUTHOR'S DECLARATION	ii
Abstract	iii
Acknowledgements.....	iv
Dedication	v
Table of Contents	vi
List of Figures	viii
List of Tables	x
Chapter 1	1
1.1 Introduction.....	1
1.1.1 Thesis Contribution.....	2
Chapter 2	4
2.1 Block Copolymers	4
2.1.1 Block Copolymer Self-Assembly	5
2.1.2 Key Components of Self Assembly	6
Chapter 3	8
3.1 Block Copolymer Thin-Films	8
3.1.1 Thin Film Deposition.....	8
3.1.2 Block Copolymer Thin Films Wettability	9
3.1.3 BCP Morphologies in Thin Film	10
3.1.4 Controlling The Out-of-Plane Orientation.....	13
3.1.5 PS-b-PMMA Thin Film	21
Chapter 4	23
4.1 Block Copolymer Lithography	23
4.1.1 Dry Etching.....	23
4.2 Fundamentals of Electron Beam Lithography	25
4.2.1 Electron Transport	26
4.2.2 EBL Resists.....	28
4.2.3 Resist Development	30
4.2.4 Process Parameters.....	31

Chapter 5	32
5.1 Experimental Work and Results	32
5.1.1 Coating PS-b-PMMA BCP Thin Film	32
5.1.2 Coating PS-b-PMMA BCP Thin Film With a Surface Neutralizing Underlayer	35
5.1.3 Different Annealing Temperature For The Self Assembly Of BCP	39
5.1.4 Different Annealing Time For The Self Assembly Of BCP	44
5.1.5 Induced Morphologies On The Same BCP Thin Film By EBL	49
Chapter 6	53
6.1 Discussion	53
6.1.1 Coating PS-b-PMMA BCP Thin Film	53
6.1.2 Coating PS-b-PMMA BCP Thin Film With a Surface Neutralizing Underlayer	53
6.1.3 Different Annealing Temperature For The Self Assembly Of BCP	54
6.1.4 Different Annealing Time For The Self Assembly Of BCP	55
6.1.5 Induced Morphologies On The Same BCP Thin Film By EBL	55
References	57

List of Figures

Figure 1: Different classes of copolymers. 1) Homo-polymer. 2) An alternating arrangement of A and B monomers, Alternating copolymer. 3) Random arrangement of monomers A and B in the chain, Random copolymer. 4) Sequential arrangement of blocks of A and B monomers, Block copolymer. 5) Attachment of side chain polymer to a backbone polymer, Graft polymer.	4
Figure 2: Formation of different micro-phase domains in a block copolymer mix.	5
Figure 3: Preferential wetting of the substrate. 1) Lamellae structure parallel to the substrate. 2) Lamellae structure perpendicular to the substrate.	10
Figure 4: Schematics of symmetric and asymmetric wetting of the substrate for the lamellar phase. .	12
Figure 5: Induced upright orientation for a corrugated surface.	15
Figure 6: Schematic of high-density nanowire fabrication in a polymer matrix. (a) An asymmetric diblock copolymer annealed above T_g under an applied electric field, forming a hexagonal array of cylinders oriented normal to the film surface. (b) After removal of the minor component, a nanoporous film is formed. (c) By electrodeposition, nanowires can be grown in the porous template.	16
Figure 7: Thickness gradient of poly(styrene- <i>b</i> -butadiene- <i>b</i> -styrene) triblock copolymer. Parts (a) and (b) are phase SPM images of the triblock copolymer which reconstructs as a function of film thickness. Part (c) is a schematic height profile of the phase images shown above, while part (d) is a simulation of the same block copolymer.	18
Figure 8: Chemical structure of PMMA- <i>b</i> -PS.	21
Figure 9: Pattern transfer using the PS- <i>b</i> -PMMA block copolymer as an etching mask.	25
Figure 10: Polymer scission from the exposure to e-beam. A) sub-unit of PMMA after the exposure to e-beam, B) High energy electron interaction with the polymer chain, and breaking of the long chain.	29
Figure 11: Distribution of PMMA fragment sizes as a function of exposure dose.	30
Figure 12: SEM image of coated PS- <i>b</i> -PMMA BCP on untreated silicon substrate.	34
Figure 13: SEM image of coated PS- <i>b</i> -PMMA BCP on untreated silicon substrate.	34
Figure 14: Schematic of 3MPTS molecule.	36
Figure 15: Schematic of PS- <i>b</i> -PMMA BCP.	36

Figure 16: AFM image of the perpendicular self-assembled lamellar PS-b-PMMA with monolayer of 3MPTS as an underlayer.	37
Figure 17: SEM image of the self assembled upright BCP lamellar structure on 3-MPTS treated silicon wafer with low coverage of 3MPTS.	38
Figure 18: AFM image of the self assembled upright BCP lamellar structure on 3-MPTS treated silicon wafer with high coverage of 3MPTS.	39
Figure 19: SEM image of the annealed BCP at 160 °C for 5min.	40
Figure 20: AFM image of the annealed BCP at 160°C for 5min.	40
Figure 21: SEM image of the annealed BCP at 190°C for 5min.	41
Figure 22: AFM image of the annealed BCP at 190°C for 5min.	41
Figure 23: SEM image of the annealed BCP at 220°C for 5min.	42
Figure 24: AFM image of the annealed BCP at 220°C for 5min.	42
Figure 25: SEM image of the annealed BCP at 250°C for 5min.	43
Figure 26: AFM image of the annealed BCP at 250°C for 5min.	43
Figure 27: SEM image of the annealed BCP at 190°C for 2min.	45
Figure 28: AFM image of the annealed BCP at 190°C for 2min.	45
Figure 29: SEM image of the annealed BCP at 190°C for 6min.	46
Figure 30: AFM image of the annealed BCP at 190°C for 6min.	46
Figure 31: SEM image of the annealed BCP at 190°C for 20min.	47
Figure 32: AFM image of the annealed BCP at 190°C for 20min.	47
Figure 33: SEM image of the annealed BCP at 190°C for 60min.	48
Figure 34: AFM image of the annealed BCP at 190°C for 60min.	48
Figure 35: SEM image of the exposed BCP thin film by e-beam.	50
Figure 36: SEM image of the exposed BCP square at $5\mu\text{C}/\text{cm}^2$	51
Figure 37: SEM image of the exposed BCP square at $12.60\mu\text{C}/\text{cm}^2$	52
Figure 38: SEM image of the exposed BCP square at $40\mu\text{C}/\text{cm}^2$	52
Figure 39: SEM image of exposed PS-b-PMMA BCP by e-beam.	56
Figure 40: SEM image of exposed PS-b-PMMA BCP by e-beam. a) Non-exposed area which shows the well defined finger print patterns. b) Exposed area by e-beam which shows morphologies other than finger print.	56

List of Tables

Table 1: Summary of common methods to orient the micro domains later and/or perpendicular to the substrate surface.....	20
Table 2: Flory–Huggins parameter for different BCPs.....	22
Table 3: Parameters affecting the EBL process.....	31

Chapter 1

1.1 Introduction

In the recent years miniaturization of semiconductor devices has slowed down due to the limits of commercial lithography technologies. The state-of-the-art immersion technology is now limited to ~22nm feature size [1]. Hence, new alternative fabrication technologies need to be developed in order to keep up with the Moores Law and further miniaturization. Although, there are some top down technologies that can fabricate feature sizes smaller than 22nm i.e. e-beam lithography. But, they are not appealing to the industry for large production, because of their low throughput, high cost, and small scale processing. A viable alternative to the top-down nanofabrication method is the bottom-up method. Where, instead of deposition and etching to sculpt the desired structures, one uses the chemical properties of the materials to form the desired structures by the self assembly of the molecules. Block Copolymer (BCP) self assembly has attracted many attentions in the past two decades and is being studied by many scientists in hope of achieving better results for nanolithography, nanotemplating, nanoporus memberanes, and ultra high density storage media [2]. Some groups have reported feature sizes down to 3nm by the use of BCP self assembly techniques [3], and efforts are being made to even further miniaturize the feature sizes down to sub-nanometer scale [4].

Although, IBM [4], and HGST [4] have announced the first manufacturing application of BCP self assembly in a conventional chip fabrication line. However, there are many challenges associated with the usage of BCPs for nanofabrication. Following are some of the more prominent challenges of BCPs: 1) In general, BCPs self assemble in an isotropic manner in the

absence of surface forces and external fields [5,6]. 2) There are very few self assemble BCP who can reach domains that are smaller than 10nm and still maintain their properties [3]. 3) They are very good for high throughput and large scale device fabrication for industrial use. However, many BCPs annealing process takes hours to days and limit this technology for commercial use [3]. 4) Achieving directed self assembled structure can be very expensive due to the high cost of instruments and processing setups such as e-beam lithography, which requires a large amount of capital and is very time consuming when it comes to fabrication of large area structure [3].

Many groups have set to tackle the above mentioned challenges and have developed different technologies to direct the self assembly of BCP film. Among which, graphoepitaxy, chemical pre patterning, solvent annealing, mechanical flow fields, electric or magnetic fields, thermal gradients, and salt doping or homopolymer blending [3], and surface wettability control [7] have shown promising results. In this work we will be focusing on a novel surface neutralization method to control the morphology and direction of the micro-domains. Furthermore, by employing e-beam lithography and using the results from the surface neutralizing method it was shown that thin film of BCP can be processed to have controlled areas of micro-domains with different morphologies.

1.1.1 Thesis Contribution

Chemical modification of the substrate surface with a self-assembled monolayer (SAM) neutral to both components of a diblock copolymer is an effective way to create

perpendicular structures to the surface of the substrate [7]. In this paper, a novel method to modify the surface energy of the substrate and to promote the formation of the perpendicular structures to the surface of the substrate is introduced. Further, efforts have been made to transfer the self assembled patterns onto to the substrate. An additional study was done to produce multiple patterns on the same BCP film by the use of E-beam lithography. The specific contributions of this thesis paper are listed below:

- 1) Novel surface treating method to neutralize the surface energy and to control the BCP's orientation and morphology. SAMs monolayer of 3MPTS polymer was evaporated on the substrate to wet both blocks of the BCP thin film.
- 2) Study of PS-b-PMMA morphology under different temperatures and time.
- 3) Controlling and modifying the BCP thin film properties by the use of e-beam lithography to produce a film with different morphologies.

Chapter 2

2.1 Block Copolymers

By representing two different monomers A and B in figure 1 and different arrangements of the AB monomers we can organize the copolymers in 4 general classes. When a single monomer is polymerized into a macromolecule, the product is called a *homopolymer* as is depicted in figure 1.(1). When the two monomers (A and B), alternate in a regular fashion along the polymer chain they produce an *alternating copolymer* as it is depicted in figure 1.(2). The copolymer with relatively random distribution of the monomers (A and B) or repeat unit in its structure is called the *random copolymer* as is depicted in figure 1.(3). A linear polymer with one or more long uninterrupted sequences of each monomer (A or B) in the chain is called the *block copolymer* (BCP) which is the basis of this paper and is depicted in figure 1.(4). *Graft copolymer* is another class of copolymers which has a black bone polymer (A) and one or more side chains of other polymers (B) and is depicted in figure 1.(5).



Figure 1: Different classes of copolymers. 1) Homo-polymer. 2) An alternating arrangement of A and B monomers, Alternating copolymer. 3) Random arrangement of monomers A and B in the

chain, Random copolymer. 4) Sequential arrangement of blocks of A and B monomers, Block copolymer. 5) Attachment of side chain polymer to a backbone polymer, Graft polymer.

2.1.1 Block Copolymer Self-Assembly

If two polymers are combined together, they will undergo phase separation on the macroscale, this is because of the unfavorable entropy of mixing between the two chains of the macromolecule. In another word, a polymer chain is comprised of chemically connected, mutually immiscible or incompatible blocks, when mixed it with another polymer chain they undergo what is termed micro-phase separation [8] and create nanoscale domains. At a certain volume fractions and polymer chain lengths, these nanoscale structures can form variety of periodic structures shown in figure 2.

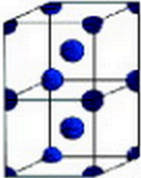
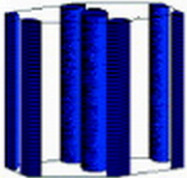
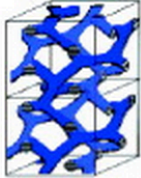
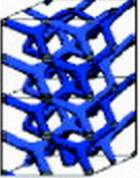

Nature of patterns	Spheres (SPH) (3D)	Cylinders (CYL) (2D)	Double gyroid (DG) (3D)	Double diamond (DD) (3D)	Lamellae (LAM) (1D)
Space group	$Im\bar{3}m$	$p6mm$	$Ia\bar{3}d$	$Pn\bar{3}m$	pm
Blue domains: A block					
Volume fraction of A block	0-21%	21-33%	33-37%		37-50%

Figure 2: Formation of different micro-phase domains in a block copolymer mix [14].

As it is shown in figure 2, shape of these micro domains primarily depends on the volume

fraction (f) of the polymer blocks. By adjusting the volume fraction of the polymer blocks one can obtain one of the following shapes: spherical, cylindrical, gyroid, diamond, and lamellar. Thin films containing these microdomain structures can then be used as nanolithographic etch masks to create dot or line patterns on solid surfaces. Similarly, size of these micro domains is determined by the molecular weight (MW) of the BCP chain. Since the polymer chains are covalently bonded together, the size scale of the domains should be proportional to the size of the polymer chain, typically on the tens of nanometres length scale or less [9].

2.1.2 Key Components of Self Assembly

Self assembly of the BCPs is best described by the Flory-Huggins equation [10]:

$$\frac{\Delta G_{\text{mix}}}{k_b T} = \frac{1}{N_A} \ln(f_A) + \frac{1}{N_B} \ln(f_B) + f_A f_B \chi \quad (1)$$

Where, ΔG_{mix} is the Gibbs free energy of mixing, k_b is the Boltzmann constant, T is the temperature, N_A is the degree of polymerization for the polymer A, and N_B is the degree of polymerization for the polymer B, f_A is the fraction composition of polymer A, and f_B is the fraction composition of polymer B, χ is the A-B Flory-Huggins interaction parameter. As it is evident in equation 1 the Gibbs free energy of the system, which dictates whether BCPs phase separate or not, is directly proportional to the degree of polymerization (N), volume fraction of the polymers (f), and the Flory-Huggins interaction parameter (χ).

The likelihood for block copolymers to phase separate into periodic micro-domains is determined by the strength of the repulsive interaction as characterized by the product χN .

Micro-phase separation can occur when this value exceeds the critical value of $\chi N > 10.5$ for the order-disorder transition [11]. If $\chi N < 10.5$, then the blocks of the BCP will mix, forming a homogeneous or phase-mixed morphology [11]. So, to decrease the size of the micro-domains and maintain a microphase-separated morphology, N must decrease and χ must increase to compensate.

Chapter 3

3.1 Block Copolymer Thin-Films

Up to this point we have been looking at the properties of BCPs in bulk. However, in order to utilize BCPs in fabrication of nanostructures we need to be able to deposit thin film of BCP on a substrate for the variety of applications such as: nanowire arrays, patterned magnetic media, and photonic crystal wave guides [12]. BCP thin film is subject to strong boundary conditions from the substrate surface and the air-polymer interface [13], and since block copolymer assembly is highly dependent on surface energies these boundaries can effectively dictate the orientation of nano-domains that were previously discussed in the thin film of BCP [13].

3.1.1 Thin Film Deposition

There are variety of methods for coating BCP film on a substrate, some common methods are: 1) Drop casting, BCP is dissolved in a solvent and a drop of liquid is placed on top of the substrate to dry, this method will leave drying spots and give non-uniform coverage. 2) Dip coating, in this method substrate is dipped into the BCP solution and is pulled out to be covered by a thin film of BCP after solvent evaporation, this method does not allow for a good control of film thickness and it results in non-uniform coverage. 3) Spin coating, is the most common method for coating of BCP on a substrate. In this methods drops of BCP solution are dispensed on top the substrate and spun at $\sim 1000-5000$ rpm [11] to obtain thin film of BCP with very uniform and homogenous coverage. Film thickness is controlled by the spinning speed,

concentration of the solution and molecular weight of the BCP. Typically, after BCP coating, films are annealed so the solvent is driven away from the film and also it allows the polymer segments to move and phase separate faster.

3.1.2 Block Copolymer Thin Films Wettability

For different applications of nanofabrication and template fabrication, it is crucial to form structures that are vertical to the substrate surface. In achieving this, we need to consider the preferential wetting of the polymeric blocks. In a hypothetical case as shown in figure 3, A-b-B BCP is spin coated on a substrate with a final goal to achieve lamellae structure. However, there are two possibilities for the lamellae structure to orient itself, either vertical or horizontal to the substrate surface. In order to achieve horizontal lamellae orientation, substrate must have a preferential wetting affinity for one the polymeric blocks (either A or B). In this case, the preferred block will first attach itself to the substrate and the other block will follow the same direction as the underlying block. figure 3.1 shows the preferential wetting of block B and its horizontal orientation. It's important to note that if block A was preferred by the substrate it would attach to the substrate first and would reverse the ordering of the polymers in the horizontal orientation (Block A would attach first then B).

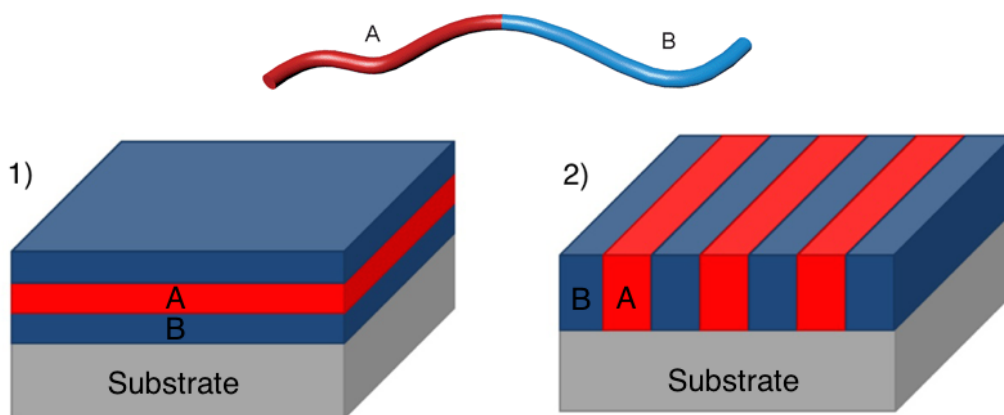


Figure 3: Preferential wetting of the substrate. 1) Lamellae structure parallel to the substrate. 2) Lamellae structure perpendicular to the substrate.

To achieve the vertical lamellae, both blocks must have a similar affinity for wetting the substrate. In other words, the substrate should almost exhibit a neutral surface energy, so the polymer blocks (A and B) will have an equal opportunity to wet the substrate, only under this condition a vertical orientation is possible as shown in figure 3.2. The key factors that control the wetting characteristic of a substrate are: a) composition, b) hydrophobicity and hydrophilicity, c) surface charges [13]. All these factors affect the surface energy of the substrate and the wetting affinity of the BCPs. In chapter 5, a novel surface energy modification method is utilized to neutralize the surface energy of the silicon substrate, and to promote the vertical alignment of the BCP micro-domains.

3.1.3 BCP Morphologies in Thin Film

In thin films, formation of morphologies primarily depends on two factors: 1) interaction of the film with the entrapping interfaces (air/substrate), and 2) compatibility of periodicity of the BCP blocks with the film thickness [14]. In contrast to the bulk BCPs, in thin

films that are thick enough to accommodate multiple domain layers the micro-domains do not follow the same pattern near the interfaces of the film. the interlayer spacing can be affected especially in the layers closest to the interfaces bounding the thin film (Air/Substrate). In this section, we present the effect of these two factors on formation of different BCP morphologies in thin films.

Lamellae morphology in thin films: In this morphology each interface (air/substrate) has affinity to wet one of the block copolymers, therefore, the block with the higher affinity for that surface will align itself parallel to the respective interface and forms the lamellae morphology. For the symmetric wetting condition where, the same block wets both surfaces, figure 4.a, film thicknesses (d) must be quantized to integer multiples (n) of the lamellae spacing (L_0), $d = nL_0$ [14]. However, for the asymmetric wetting where, the two surfaces are not wetted by the same block figure 4.b, film thicknesses must quantize to $d = (n+1/2)L_0$ [14]. If the film thickness does not follow these conditions, then Islands and holes (or “Terraces”) will form[14]. This is because the energetic penalty for creating more film surface area is less than the penalty caused by altering the domain periodicity (chain stretching or compression) or by putting an energetically disfavored block in contact with one or both surfaces [15]. If $d < L_0$, perpendicular morphologies are possible [15].

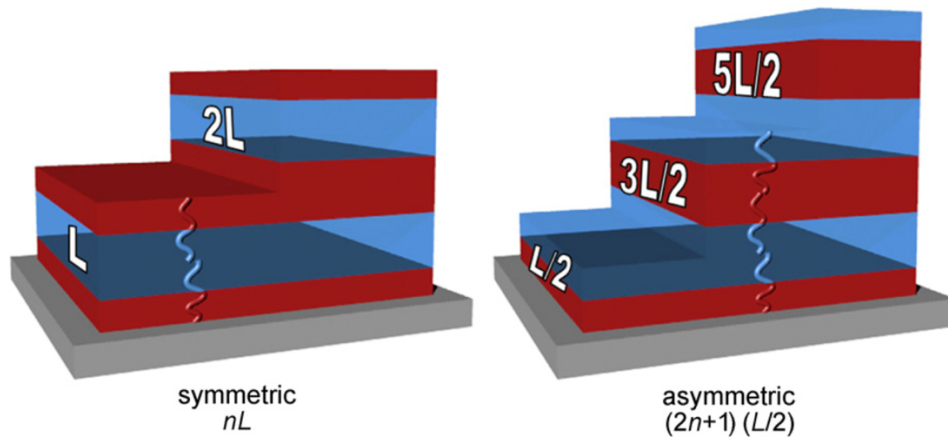


Figure 4: Schematics of symmetric and asymmetric wetting of the substrate for the lamellar phase.

Cylindrical morphology in thin films: Just like the lamellae phase, the preferential wetting of the substrate by one of the blocks will orient the cylinders parallel to the surface. If the surface has higher affinity for the minority block, then a brush like structures (perpendicular cylinders) will form [15]. Similarly, for the cylindrical phase, discrete film thicknesses are allowed. If the thickness does not follow the discrete thicknesses then interesting morphologies such as perpendicularly oriented cylinders and perforated lamellar structures form [15]. At certain thicknesses the cylindrical morphology will transition to a close-packed spherical morphology because of the high energy cost of distorting the cylinders away from their preferred spacing [15].

Spherical morphology in thin films: If the minority block wets the surface micro domains will stack themselves parallel to the surface. In bulk, the spheres pack into a *bcc* lattice, however in thin films, a monolayer of spheres packs into a close-packed configuration, which may be viewed as a distorted $\langle 1\ 1\ 0 \rangle$ plane of the *bcc* structure, as there are no longer any neighboring layers to break the in-plane symmetry [15].

3.1.4 Controlling The Out-of-Plane Orientation

The orientation of the micro domains in BCP thin films are very important in the applications of nanofabrication. In the case of dry etching which is widely used to pattern transfer [3, 11], in order to achieve a certain etch depth, the thickness of the etching mask and the selectivity of the mask compared to the substrate material is very crucial. Micro domains with upright orientation give a better control for etching, because they have a high aspect ratio and are better for pattern transfer. However, forming micro-domains with perpendicular orientation is very challenging, because naturally block components of BCPs have different affinity for the bounding interfaces (air/substrate) and this preferential wetting mechanism as we have discussed in the previous section leads to parallel orientation of the domains rather than the perpendicular orientation. In order to reach this unique orientation blocks must not show preferential affinity for either surface. In this section we present some of the most common and effective ways to reduce the surface energy in order to reach the perpendicular orientation.

3.1.4.1 Neutralization By The Use of Monolayers

Many groups have reported the neutralization of the surface by employing different monolayers of material as a primer for the BCP film. A common method is to graft a random block copolymer to the surface of the substrate, this step will ensure that surface energy is neutralized and the substrate has an equal affinity for both blocks, hence promotion of the perpendicular orientation of the micro-domains. Mansky et al. found the optimal PS content

(~60%) in a PS-*r*-PMMA copolymer to neutralize the surface for a lamellae-forming PS-*b*-PMMA [16, 17]. Han et al. later showed that the range of PS content in the random copolymer yielding perpendicular cylinders for PS-*b*-PMMA was slightly different than the range yielding perpendicular lamellae [18]. Peters et al. used self-assembled monolayers of octadecyltrichlorosilane (OTS) that were chemically altered by X rays in the presence of air to generate aldehyde and hydroxyl groups which, at the proper level, can yield a neutral surface for PS-*b*-PMMA [19]. Kim et al. used self assembled monolayer (SAM) of silanes on silicon substrate to reduce the surface energy and successfully induced the upright orientation of the BCP lamellae and cylindrical morphologies [20]. In our work we will employ similar technique to Kim's method which will be discussed in more details in the later chapters.

3.1.4.2 Corrugated Surfaces

Rough surfaces can also promote the upright orientation, this is because penalty is incurred for elastic deformation to conform to a rough substrate, Sivaniah et al. observed perpendicular orientations in lamellae-forming PS-*b*-PMMA on a rough substrate [21]. Also, chemically patterned surfaces have been generated that have periodic affinities to each block, which causes a lamellae-forming block copolymer to orient perpendicularly to the surface [15]. Figure 5.a shows the AFM image of diblock copolymer with upright morphology on corrugated substrate. Figure 5.b and c. are representation of the underlying mechanism for the lateral orientation of the micro-domains on corrugated substrate.

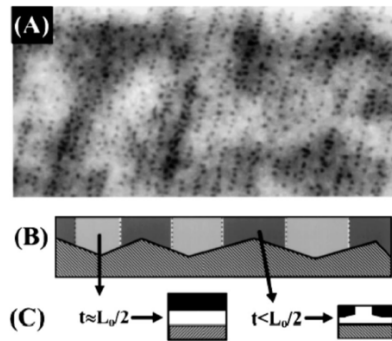


Figure 5: Induced upright orientation for a corrugated surface [11].

3.1.4.3 Addition of Additives In The BCP

This reorientation is due to segregation of the additive particles at the interface and mediate the block copolymer/substrate interactions. Lin et al. added cadmium selenide nanoparticles to a cylinder-forming PS-*b*-P2VP block copolymer, which caused reorientation of the microdomains perpendicular to the substrate [22]. A cylinder-forming blend of PS-*b*-PMMA with poly(ethyleneoxide)-coated gold nanoparticles (Au-PEO) can be induced to orient perpendicular to the substrate by annealing in humid air [23]. Jeong et al. showed that addition of dry-brush PMMA homopolymer to a cylinder-forming PS-*b*-PMMA block copolymer will stabilize the perpendicular orientation of the microdomains in thicker films (hundreds of nanometers) [24]. Wang et al. induced a perpendicular orientation of a lamellae-forming block copolymer by adding lithium chloride to PS-*b*-PMMA [25].

3.1.4.4 Applying External Forces

Another method to reorient the micro-domains into perpendicular orientation is by

applying electric field to the BCP thin film. Thurn-Albrecht et al. have demonstrated the use of electric fields in orienting cylinder-forming PS-*b*-PMMA block copolymers perpendicular to the substrate, as sufficient contrast in dielectric permittivity exists between these two blocks [26]. In their experiment, electric field was applied to BCP film which, was bounded in between two aluminum electrode with Kapton spacer to avoid shorting [26], figure 6 represent the schematic of the setup. They have managed to measure the minimum voltage required to achieve upright micro-domains in films with up to 30um [26]. Xu et al. were able to align lamellae-forming PS-*b*-PMMA with an electric field, although not for all thicknesses (thin films stubbornly remained parallel, whereas very thick films, $>10L_0$, had parallel orientations near their surfaces) [27].

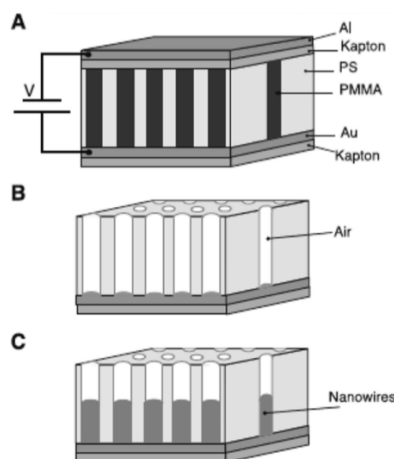


Figure 6: Schematic of high-density nanowire fabrication in a polymer matrix. (a) An asymmetric diblock copolymer annealed above T_g under an applied electric field, forming a hexagonal array of cylinders oriented normal to the film surface. (b) After removal of the minor component, a nanoporous film is formed. (c) By electrodeposition, nanowires can be grown in the porous template [26].

In thin films, the electric field is useful for fabricating micro-domains oriented perpendicular to the substrate with high aspect ratio.

3.1.4.5 Solvent Casting of The Block Copolymers

In this method micro-domains align themselves perpendicular to the substrate because of solvent evaporation is very directional, solvent evaporation rate is one of the key factors that determines the orientation of the domains [15]. Another characteristic of this method is that in general solvents promote the mobility of the blocks and speed up the grain growth [15]. Even though, there has been multiple reports for orienting micro-domain employing this method, A careful temperature control, vapor pressure, vapor extraction speed make this method very difficult to use. Moreover, due to the uniaxial degeneracy of perpendicular lamellae and vertically oriented cylinders, this approach cannot result in a good lateral order [15].

3.1.4.6 Thickness Gradient

As it was discussed in section 3.1.3 lamellae structures have a natural repeat spacing of the domain structure of nL_0 for the symmetric wetting condition, and $(n+1/2)L_0$ for the asymmetric wetting condition. We've also learned that if the film thickness is not commensurate with this spacing a series of islands and holes will form. So when the film is spun on the substrate is the film thickness matches the natural thickness of the BCP polymer then a smooth surface is visible for the case of parallel orientation of the BCP film, however if the film thickness does not follow the nL_0 criteria for the symmetric wetting and $(n+1/2)L_0$ for asymmetric wetting, then lamellae phase with perpendicular orientation will form. In sphere and cylinder forming block copolymers, islands and holes form when the film thickness does not closely match a natural thickness given approximately by $h = an + b$, where a is the sphere

(or cylinder) layer-to-layer distance and b is the thickness of the brush adsorbed on the surfaces (if such a brush forms) [28]. Figure 7 helps to visualize the thickness gradient of the BCPs. In it, surface reconstructions of a cylindrical block copolymer including reorientation of nanodomains, wetting layers, and perforated lamellae is clearly observable and this because of the interplay between surface fields and confinement effects [28].

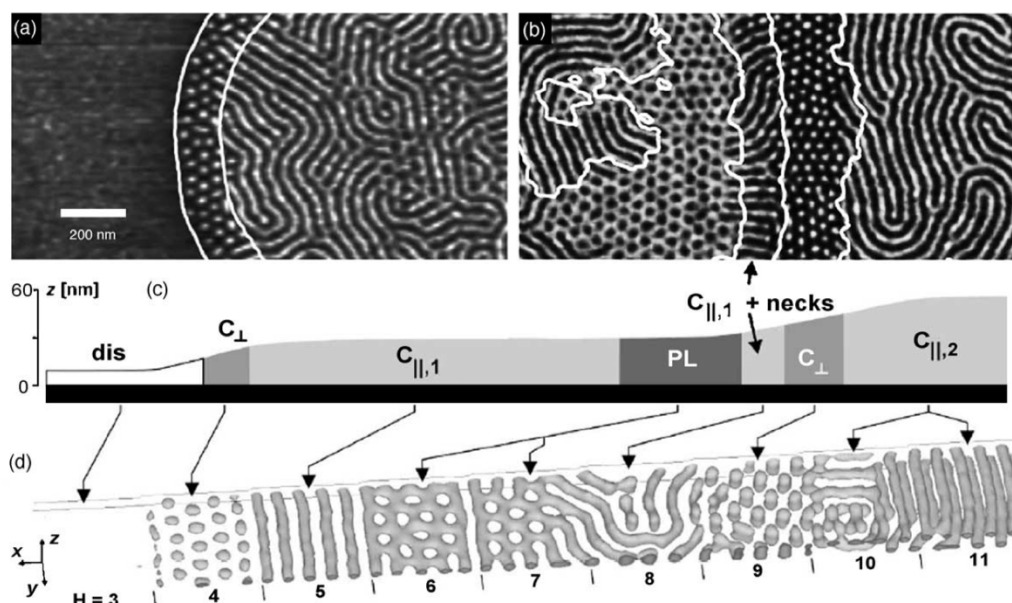


Figure 7: Thickness gradient of poly(styrene-*b*-butadiene-*b*-styrene) triblock copolymer. Parts (a) and (b) are phase SPM images of the triblock copolymer which reconstructs as a function of film thickness. Part (c) is a schematic height profile of the phase images shown above, while part (d) is a simulation of the same block copolymer [28].

3.1.4.7 Mechanical Flow Fields

An interesting mechanism for aligning the BCP domains is to use shearing forces to orient the micro-domains. Albalak et al. [30] used roll-casting, wherein a block copolymer solution is allowed to evaporate while an extensional flow is induced between two co-rotating

rolls to orient cylinders and lamellae parallel to the extension direction [30]. This method produced films with high thickness of 30um, however other methods were developed to obtain film with lower thicknesses. Kimura et al. [31] used the flow of a droplet pinned to a tilted surface in conjunction with solvent evaporation to orient a cylinder forming PS-*b*-PB thin film [31]. The pinning of the drop causes directional flow within the droplet normal to the pinned edge, which induces ordering as the solvent evaporates. Another variation of this method is to use sphere forming BCP to create cylindrical micro-domains, in this method sphere forming BCP, which is close to the sphere/cylinder phase boundary is put under the shear force to transform the spheres into cylinders along the direction of the applied force [32].

3.1.4.8 Temperature Gradient

Berry et al. [33] developed a method in which a temperature just below the order disorder temperature and above the glass transition temperature of PS-*b*-PMMA was applied to the BCP film in the direction of the front motion on a rolling substrate. Temperature gradient was created by passing the sample (at a controllable rate) across a hot block between two cold blocks, which creates a bell-shaped temperature profile for each spot in the film as a function of time. This resulted a more rapid motion of the defects and increased reorientation of the micro-domains as the velocity of the sample decreased [33]. They attribute the ordering to the creation of an in-plane spatiotemporal mobility gradient that biases the grains as they form [33].

Table 1 summarizes the most common methods to orient the micro-domains in an upright position for both bulk and thin film forms. In general, these methods are bottom up approach and fall under the self assembly mythology. There are other methods which produce better and more controllable orientations such as: epitaxy, directional crystallization of a solvent-polymer solution, and graphoepitaxy, but these methods rely on pre-patterning of the substrate with various lithography techniques, and they can not be categorize under the full self assembly orientation of the BCP, and therefore are beyond the scope of this report.

Table 1: Summary of common methods to orient the micro domains later and/or perpendicular to the substrate surface [14].

Interactions	Driving forces	Experimental methods	Characteristics	Type of sample
Mechanical flow fields	Shear and elongation	Extrusion	Easy control, large samples	Bulk
	Shear	Rheometer	Easy control of parameters	Bulk
	Compression	Channel die	Simple apparatus	Bulk
	Shear and elongation	Roll casting	Ordering from solution	Bulk
	Elongation	Petermann method	Semicrystalline BCP	Thin films
Temperature gradient	Temperature gradient	Zone refining cell	High degree of orientation, slow process	Bulk
Electric field	Dielectric contrast	In-plane and vertical	Low degree of orientation lack of lateral orientation	Bulk/thin films
Surface tension	Surface tension	Spreading on a fluid surface	Liquid crystalline/semicrystalline BCP	Thin films
Thickness and substrate	Commensurability	Thickness control	Parallel/vertical LAM, CYL	Thin films
	Preferential wetting	Confinement	Only parallel ordering	
	Neutral substrate	Random copolymer	Vertical LAM, CYL w/o lateral order	
Special block copolymers	Architecture	Spin coating	Vertical LAM w/o lateral order	Thin films
	Liquid crystallization		Vertical LAM w/o lateral order	
	Crystallization and wetting/dewetting		Vertical LAM w lateral order near wet./dewet. boundary	
Solvent control	Evaporation rate	Spin coating	Vertical CYL w slow evap. rate	Thin films
	Prewetting		In-plane CYL near rims	
Patterned substrates	Chemical pattern	Soft lithography	Vertical/parallel LAM	Thin films
	Topographic pattern	Silicon miscut	Vertical LAM	
		Holographic pattern	Conformal/anticonformal	
		Softlithography	Micromolding	
	Chemical/topographic	Silicon miscut/metal deposition	Vertical LAM	

3.1.5 PS-b-PMMA Thin Film

Though, there are many different block copolymers available, we have focused our attention to PS-b-PMMA (poly (styrene) and poly (methyl methacrylate)) block copolymer due to variety of reasons. Figure 7 depicts the chemical structure of the PS-b-PMMA block copolymer.

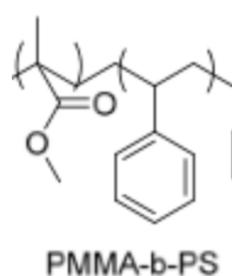


Figure 8: Chemical structure of PMMA-b-PS.

There are variety of good reasons for why the PS-b-PMMA block copolymer is used in this study. First, PS-*b*-PMMA is readily available as a commercial BCP. Second, it has narrow molecular weight distributions of each block. Third, PMMA is a standard photoresist and a PS is negative e-beam resist. Fourth, the surface energies of PS and PMMA are very similar which make it easier to control the orientation of the nano-domains within the film [9]. Fifth, PS-*b*-PMMA has a small Flory-Huggins interaction parameter (~ 0.043 at 25C) compared to the other BCPs as listed in table 2. These properties of PS-*b*-PMMA make it a great candidate for nanolithography and pattern transfer applications. Thurn-Albrecht *et al.* [9] first reported the application of PS-*b*-PMMA to fabricate a porous polymer template. In their method they degraded the PMMA block by exposing it to the UV light, and cross linking the PS block.

Further, they developed (removed the PMMA block) the pattern by the use of Acetic Acid, which resulted in a nanoporous template on top of their substrate.

Table 2: Flory–Huggins parameter for different BCPs [9].

polymer name	Flory–Huggins		
	parameter	χ at 25°C	χ at 180°C
PS- <i>b</i> -PMMA [57]	$4.46 T^{-1} + 0.028$	~ 0.043	~ 0.038
PS- <i>b</i> -PEO [58]	$29.8 T^{-1} - 0.023$	~ 0.077	~ 0.043
PS- <i>b</i> -PI [59]	$33 T^{-1} - 0.0228$	~ 0.088	~ 0.050
PS- <i>b</i> -P2VP [60]	$63 T^{-1} - 0.033$	~ 0.178	~ 0.106
PS- <i>b</i> -PLA [61]	$98.1 T^{-1} - 0.112$	~ 0.217	~ 0.105
PS- <i>b</i> -PDMS [58]	$68 T^{-1} + 0.037$	~ 0.265	~ 0.187
PTMSS- <i>b</i> -PLA [62]	$51.3 T^{-1} + 0.29$	~ 0.478	~ 0.403
PS- <i>b</i> -PFS	n.a.	n.a.	n.a.

Chapter 4

4.1 Block Copolymer Lithography

4.1.1 Dry Etching

In the semiconductor industry dry etching is widely used to transfer the pattern on the mask to the substrate. The main reason that dry etch is used over the wet etch is that it allows for directional etching of the substrate, whereas the wet etch allows for isotropic etching of the material. In dry etching, etchant gas is ionized by high radio frequency (RF) field. An applied electric field accelerates the ions towards the substrate, these ions create a chemical reaction with the surface molecules of the substrate to physically remove the material by a sputtering mechanism. The feature size on the mask determines the lateral resolution of the transferred pattern, and the achievable depth of the etch profile is limited by the thickness of the mask material, selectivity of the etchant and fidelity of the etch.

Similar to conventional lithography techniques, in the BCP lithography a thin film of the BCP is spun coated on top of a substrate, based on the discussions in the previous chapter, BCPs can self assemble to form one the possible morphologies (spherical, lamellae, cylindrical) on the substrate. Again, a detailed explanation was presented in the previous chapters on how to achieve morphologies with upright or perpendicular orientation with respect to the substrate. Achieving high aspect ratio perpendicular morphologies are very important in BCP pattern transfer due to higher selectivity and usefulness of the patterns in nanolithography. Once, the desired morphology is reach on the surface of the substrate, Oxygen plasma is used to

selectively remove PMMA component and the underlying films, C₂F₈ and O₂ [34] are used to remove the polymer and finally SF₆ is used to etch the silicon. Figure 8 depicts the pattern transfer of the Lamellae structure into silicon substrate with an under-layer of PS-OH to neutralize the surface. Typically, to achieve periods smaller than 20nm, usually the thickness of the BCP template must be very small, this film thickness reduction limits the fidelity of the pattern transfer, due to low selectivity in the etching rate of the BCP blocks. In dry etching of BCPs oxygen gas is used to oxidize and remove the organic polymers. Since the selectivity of most BCPs are very close to each other, therefore the fidelity of the transfer can be compromised when the film thickness is low.

To solve the selectivity issue, an additional step is introduced in pattern transfer of PS-b-PMMA to stay faithful to the fidelity of the pattern transfer. Just like the pattern development process in lithography technique. In some cases, aside from the RIE, UV exposure and solvent development is employed to remove PMMA micro-domains from the PS-b-PMMA masking pattern. A film with higher selectivity is deposited on top of the PS-b-PMMA masking layer to create a negative replica of the template. Next, the new mask (usually a metal layer) with the negative pattern is used to transfer the pattern into the substrate material. Black *et al.* [8] showed that PS-b-PMMA block copolymer can be used as an etching mask to pattern transfer using the fluorine (SF₆) Reactive Ion Etching (RIE).

For silicon (Si) and metals, fluorine-based etch chemistry, using fluorinated gases, such as SF₆, C₂F₈ or CHF₃, in combination with argon (Ar) gas, are most effective [8]. The etch rates depend on the different ionization and acceleration conditions. Typically, a higher RF power increases the ion density, and, consequently, the etch rate. Ion milling, which is physical

bombardment of the substrate surface by the ions, is typically using Ar ions. Ion milling is similar to RIE, but based on a directional sputtering process.

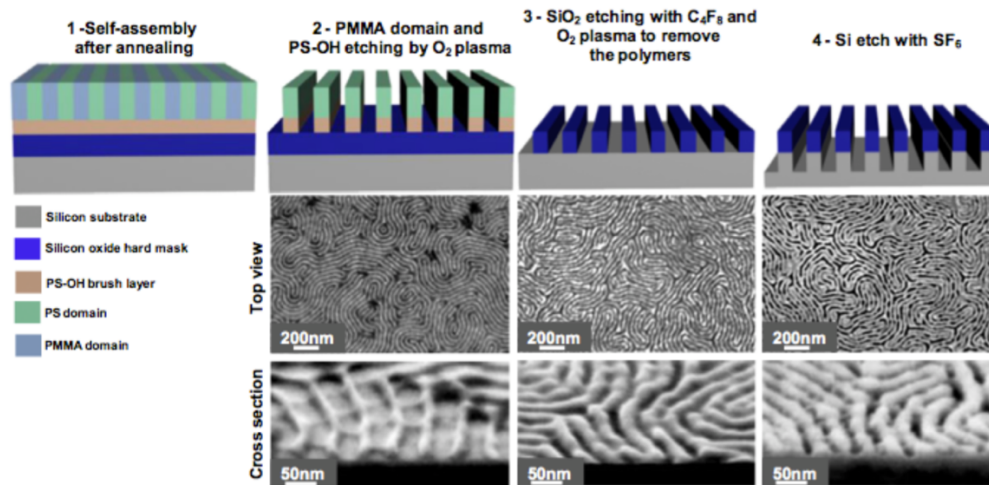


Figure 9: Pattern transfer using the PS-b-PMMA block copolymer as an etching mask [34].

4.2 Fundamentals of Electron Beam Lithography

Electron beam lithography (EBL) is one of the most popular top-down nanolithography techniques for the research and development, lithography mask production, biosensors, MEMS/NEMS, LEDs, biosensors. EBL's popularity is mainly due to its maskless processing, which reduces the fabrication cost and the fabrication capability. In e-beam lithography the main objective is to produce arbitrary patterns in the resist with high resolution, high density and high reliability. Many other applications are being developed in R&D, we will explore one of these applications in the next chapter. In general, e-beam lithography is comprised of three main steps: 1) exposure of the sensitive material (resist), 2) development of the resist and 3) pattern transfer. It is important to note that all of these steps and their sub processes are very

important in obtaining very high resolutions features. A great number of parameters are involved in each step of e-beam lithography, which contribute to the quality of the results. Choosing a right resist is very important for EBL. Among all EBL resists, Polymethyl methacrylate (PMMA) is the most popular positive resist, and is specially interesting when it is used in BCPs, because its properties can be modified and controlled by EBL. Although, PMMA is one of the first materials originally tested for EBL, but still, it remains as the most popular EBL resist, because it has high resolution and easy processing.

A more detail processing of EBL presented in the following section, however in short, EBL operates by exposing a very high sensitive resist to very narrow and focused electron beam. Due to the interaction of the electrons with the molecules of the resist, molecules either degrade (in the case of positive tone resist) or crosslink (in the case of negative tone resist). Modified molecules by the means of electron exposure can then be removed (developed) by a solvent to create structures in the resist film, further pattern transfer process will allow for the permanent pattern transfer of the structures into a substrate. The main steps in EBL lithography are discussed in more details in the subsequent sections.

4.2.1 Electron Transport

A very crucial step in EBL is electron beam formation. In order to be able to expose very fine features on the film (resist), a very stable and high quality e-beam is required. A common technology to produce this high quality e-beam is the use of thermal field emission. Beam's spot size, which is a very essential parameter in EBL, is controlled by the electron

optics that are integrated in the EBL system, and the degree to which the beam can be focused. Parameters such as stigmatism and aperture alignment are also very essential in determining the beam spot size and shape. Another, factor to obtain very stable and focused e-beam is to create high vacuum inside the e-beam chamber to reduce the scattering of the beam and electrostatic repulsion by the electrons. Most commercial EBL systems are now able to produce e-beam spot sizes down to 10nm however, there has been reports of e-beam spot size down to 2nm [35].

Once the a focused and stable beam is produced, the interaction of the electrons and the resist become important in determining the beam shape inside the resist. When electrons enter the resist they exhibit low energy elastic collision. and will deflect from their original path, this phenomenon is called the forward scattering of the e-beam. Deflection of the electrons from their original path will broaden the beam diameter inside the resist, the broadening of the beam due to forward scattering is dependent on the thickness of the film, which will reduce the resolution of the features. Aside from the forward scattering, another scattering phonon can take place inside the film called back scattering. When electrons are accelerated into the resist most of them pass through the resist and end up in the substrate, however a tiny fraction of them reflect back into the resist at some distance away from the original point of entry and will expose the resist on their journey back. This undesired exposure of the film in the vicinity of the point of first exposure is called the proximity effect and is caused due to the backward scattering of the electrons. This effect can limit the production of the dense patterns in EBL. One way to minimize this effect is to reduce the film thickness.

Another important factor about e-beam is the electrostatic charging, which needs to be taken into account when high resolutions are needed. When, electrons are accelerated towards the resist if there is no path way for the absorbed electrons to dissipate, they will start to locally accumulate in the resist or substrate and will distort the beam focus. Therefore, it is crucial to coat the resist with conductive polymers or metals to create a scape pathway for excess the electrons. This is also important when working with BCPs. It is important to deposit a conductive layer on top of the BCPs in order to be able to characterize them with SEM. Chromium was used in our studies to reduce the charging effect on the BCP.

4.2.2 EBL Resists

As we mentioned before, resist is very essential in determining the final resolution of the e-beam lithography and can be manipulated by the e-beam for different purposes. As it was mentioned in the previous section, when electrons enter the resist, they exhibit an inelastic collision with the resist and ionize the resist, which create secondary electrons. Resist ionization will lead to chemical changes in the resist, just like the typical lithography process. There are two classes of resists: 1) positive tone resist, 2) negative tone resist. In positive resist, with the most important one being PMMA, chemical properties will change by the exposure to e-beam so that the solubility of the resist changes from low to high. When exposed to e-beam, PMMA's long polymeric chains are broken into smaller fragments, this will allow the smaller fragments to be dissolved in the solvent more easily. This concept is the bases for the process we employ to create different morphologies in the BCP thin film of PS-b-PMMA. In negative resist, a reverse phenomenon happens, which means, small chains in polymer undergo

chemical overhaul to create longer chains, and become less soluble in the solvent. Among the popular negative tone resists for EBL are HSQ (hydrogen silsesquioxane), SU8, and Polystyrene (PS). Figure 10 represent the schematic process of polymer scission by the exposure to the e-beam. As it is shown in figure 10.b, high energy electron interaction with the polymer will break the bonds in the long polymeric chains and will create smaller polymeric units as it is depicted in figure 10.a.

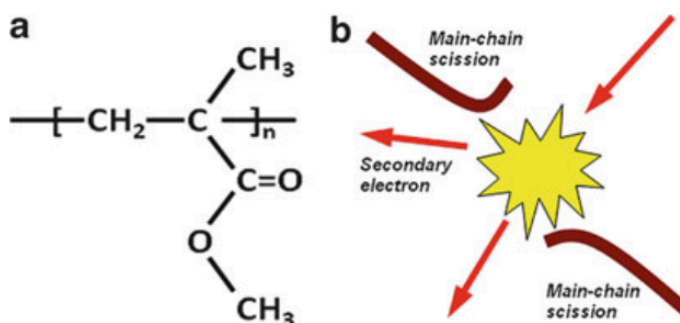


Figure 10: Polymer scission from the exposure to e-beam. A) sub-unit of PMMA after the exposure to e-beam, B) High energy electron interaction with the polymer chain, and breaking of the long chain [36].

The typical masses of PMMA polymer ranges from 496 to 950 kDa [36]. To break these long chains, many scission events are required to create small soluble fragments of the PMMA chains. In order to control the scissioning events one needs to control the exposure dose of the EBL and the development behavior of the polymer. Figure 11 shows the distribution of the fragment sizes of PMMA for different exposure doses. As it is evident in this figure, higher exposure doses create a narrower distribution, and smaller fragments, therefore higher solubility is expected. These parameters can be exploited in the formation of different BCP

morphologies, essentially by controlling the exposure dose we can control the length of the PMMA chain in the PS-b-PMMA BCP. As we have discussed earlier if the polymer fraction in the BCP mix is varied different morphologies can be obtained.

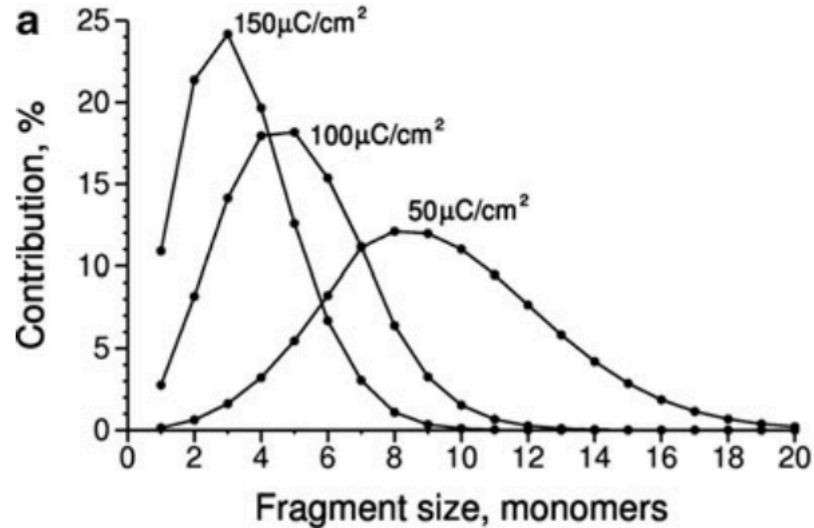


Figure 11: Distribution of PMMA fragment sizes as a function of exposure dose [36].

4.2.3 Resist Development

Once the desired pattern is exposed on the resist, the next step is to develop the resist. In this process, the exposed resist is washed away (in the case of positive resist, for the negative resist non-exposed areas will be washed) with a developer. In this process, solvent will surround the small fragmented chains of the resist polymer, and remove the polymer fragments from the original polymer matrix leaving the non-exposed areas with the negative of the original pattern. Longer polymer fragments are more strongly bonded to the matrix, therefore a longer development time and stronger developer is required to remove them from the matrix.

Exposure and development are interrelated, as short exposure with long or aggressive development can be equivalent to heavier exposure with short development [36].

4.2.4 Process Parameters

As it was mentioned previously, though there are three major steps in EBL processing. There are many other sub-categories that can effect the final resolution and results of the EBL. Table 3, summaries some of the most important factors that play a significant role in determining the final results of EBL process.

Table 3: Parameters affecting the EBL process [36].

Parameter	Process impact
Exposure energy	Resolution, sensitivity, proximity
Exposure dose	Pattern quality
Pattern density	Proximity, pattern quality
Resist material	Sensitivity, resolution, contrast
Resist thickness	Sensitivity, resolution, pattern quality
Developer	Sensitivity, resolution, development window
Development temperature	Sensitivity, resolution, exposure window
Development time	Sensitivity, resolution, exposure window

To summarize the e-beam lithography, there are three main steps involved in producing nanostructures, e-beam formation and control, e-beam/resist interaction, development and pattern transfer. The key parameters that determine the quality and resolution of the EBL are: e-beam quality and size, quality of the resist material, interaction of the developer and the resist, e-beam energy and exposure dose, development time and temperature. In this report EBL was used to manipulate the properties of PS-b-PMMA BCP in order to obtain different morphologies of BCP.

Chapter 5

5.1 Experimental Work and Results

In this chapter we will discuss the method and material used to produce perpendicular lamellar nano-domains in thin film of PS-b-PMMA block copolymer. In addition, effect of different annealing temperature and time on the lamellar forming BCP of PS-b-PMMA is studied. Further, experimental process with E-beam lithography in order to achieve multiple nano-domain morphologies on the same film of BCP is presented.

5.1.1 Coating PS-b-PMMA BCP Thin Film

In the first experiment, numerous efforts have been made to coat the silicon wafer with PS-b-PMMA copolymer. A 1:1 polymer composition of PS-b-PMMA (65.3 Kg/mol- 66.6 Kg/mol) was mixed in (1%) Toluene solvent by the Advanced Polymer Materials Inc. (APM) chemical company. The solution was spin coated (at 2000 rpm, 40 sec) on a clean silicon wafer (solvent cleaning and Oxygen RIE was done to clean the surface) and ~40nm thick film was obtained. Next, Sample was baked at 90°C for 3 minutes to drive off the solvent. The film was then annealed on a hotplate at 190°C for 20 minutes in a nitrogen glove box to drive off the defects and to obtain finger print (lamellar) morphology.

In order to check the results, the BCP was exposed to O₂ plasma, as we have discussed previously, oxygen plasma oxidizes the organic polymer which leads to the etching of the organic polymer. Exposure of the BCP to oxygen plasma for 10 second under 20 Watt RF

power, 1mTorr pressure, and 20 sccm gas flow leads to ~30nm etching of PMMA and ~10nm etching of PS. This etching process reveals the pattern on the surface of the substrate, which can then be seen either by the use of Atomic Force Microscope (AFM) or Scanning Electron Microscope (SEM). SEM images for this sample are shown in figures 12 and 13.

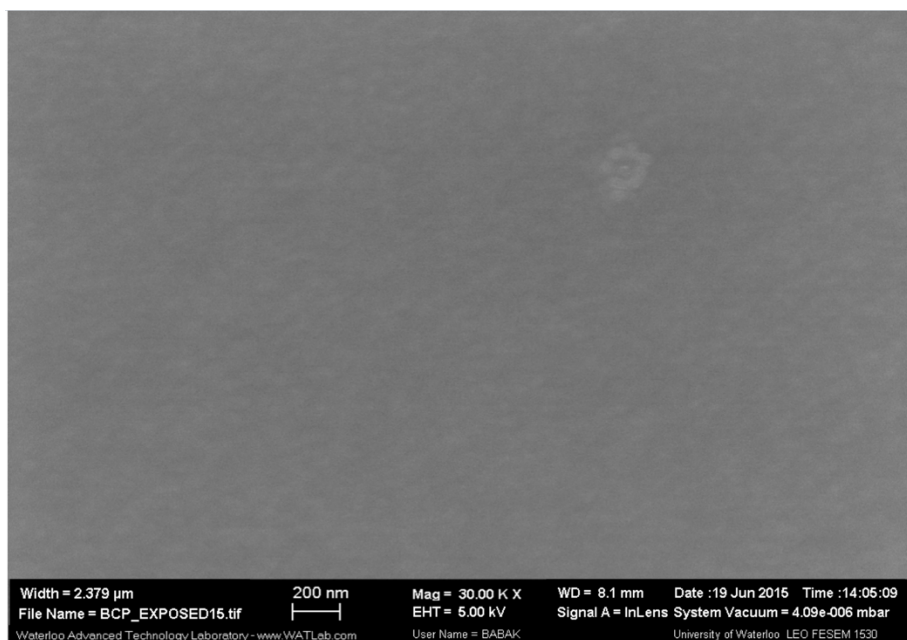


Figure 12: SEM image of coated PS-b-PMMA BCP on untreated silicon substrate.

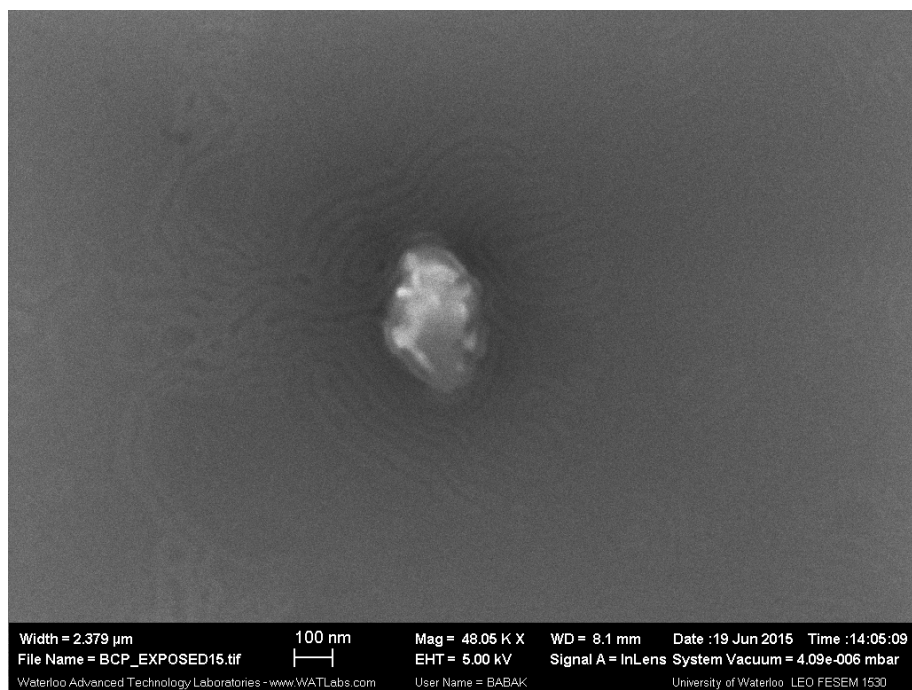


Figure 13: SEM image of coated PS-b-PMMA BCP on untreated silicon substrate.

As it is depicted in figure 12 the finger print pattern is not visible on the surface of the substrate, except around the edges of the available artifacts on the sample, which is visible in figure 13. This is not unexpected, because as we have discussed in section 3.1.4, in order to get the upright orientation for the lamellar morphology we must neutralize the surface energy of the substrate and create an equal opportunity for both blocks to attach themselves to the surface of the substrate in the upright position. Thus, as it is shown in the SEM images above it is clear that substrate has shown higher affinity to one of the blocks in the BCP mix and forced the micro-domains to align in the lateral direction, hence the flat and smooth looking images.

5.1.2 Coating PS-b-PMMA BCP Thin Film With a Surface Neutralizing Underlayer

The coating process that was used in the first trial was employed again to coat the PS-b-PMMA BCP on the silicon wafer. With an exception, that this time a surface neutralizing monolayer was deposited under the BCP layer. B.H. Sohn and S.H. Yum first reported the use of 3-(p-methoxyphenyl) propyltrichlorosilane (3-MPTS) monolayer to reduce the surface energy of the substrate in order to produce upright lamellar morphology for the PS-b-PMMA BCP [7]. They coated the 3MPTS monolayer first, then the BCP, to get very well defined and perpendicular micro-domains. Although, their method produced very good results, but their monolayer (3MPTS) coating process took 48hrs [7], which is a great issue and is not acceptable for high throughput fabrication.

In our second trial we modified B.H Sohn and S.H. Yum's method to obtain perpendicular

lamellar morphology. Prior to coating the BCP, a Self Assembled Monolayer (SAM) of 3MPTS was formed on a clean (solvent cleaning and then O₂ plasma was used) substrate by the means of evaporation. This was done by placing a 1cm x 1cm piece of silicon wafer on top of few droplets of 3MPTS in a wafer-box without allowing the substrate to touch the droplets. As shown in figure 14, 3MPTS has both phenyl and O groups. The phenyl group tends to wet the polystyrene, figure 15, and the O group tends to wet the PMMA, figure 15.

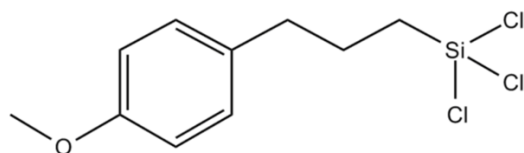


Figure 14: Schematic of 3MPTS molecule.

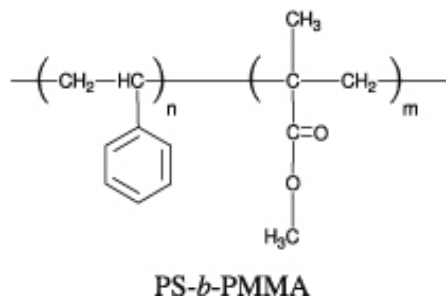


Figure 15: Schematic of PS-*b*-PMMA BCP.

This non preferential wetting of the BCP will make the 3MPTS monolayer neutral, and can allow for perpendicular orientation of the lamellar structures. The wafer was then removed from the wafer box after 2 hours, and ~40nm PS-*b*-PMMA film was spun coated on the SAM layer, followed by 3 minutes of baking at 90°C, and 20 minutes of annealing at 190°C. The same O₂ plasma as the previous trial was carried over and an AFM image was taken to see the

result. Figure 16 shows the self assembly of BCP on a 3MPTS treated silicon substrate. As it was expected very well defined upright lamellae (finger print pattern) of the BCP is visible in this image, which confirms the successful coating of the 3MPTS monolayer. As it is shown, the characteristic finger print patterns are visible with some defects and contaminants. The formation of the bubbles in the film can be caused by the trapped solvent in the film and its escape path during the baking or annealing of the film.

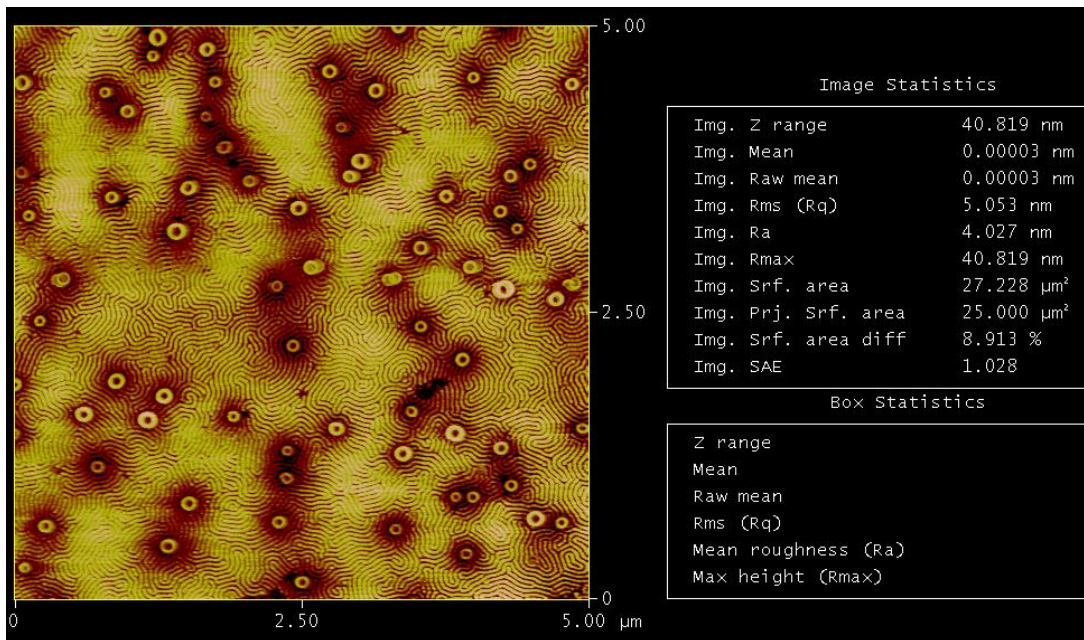


Figure 16: AFM image of the perpendicular self-assembled lamellar PS-b-PMMA with monolayer of 3MPTS as an underlayer.

Obtaining a smooth SAM of 3MPTS over an entire wafer is a very challenging task. If the optimum time and the distance between the drops and the substrate the is not reached the SAM of 3MPTS will not uniformly cover the substrate surface. This non-uniform coating of the substrate will lead to formation of the islands (patches) of lamellar structures as it is shown in

in figure 17. Areas that don't show the finger print lamellar structure exhibit preferential wetting by the substrate, hence the lateral orientation of the polymer make the film look smooth with no patterns.

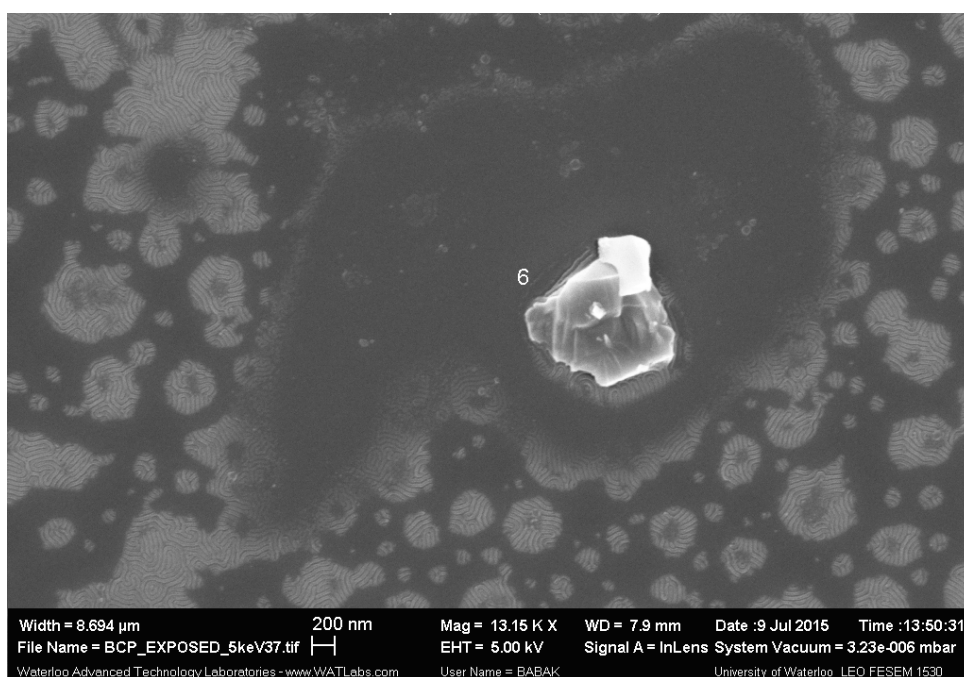


Figure 17: SEM image of the self assembled upright BCP lamellar structure on 3-MPTS treated silicon wafer with low coverage of 3MPTS.

In order to solve the uniform coating of the substrate with the 3MPTS monolayer, the experimental setup was modified in a way so that the wafer is directly above the 3MPTS droplets, with a uniform exposure to the droplets. Also, the volume of the droplets under the substrate were increase so that a greater area of the substrate would be covered by the evaporated molecules. The process was repeated and this time a uniform coverage of 3MPTS and BCP was observed as shown in figure 18.

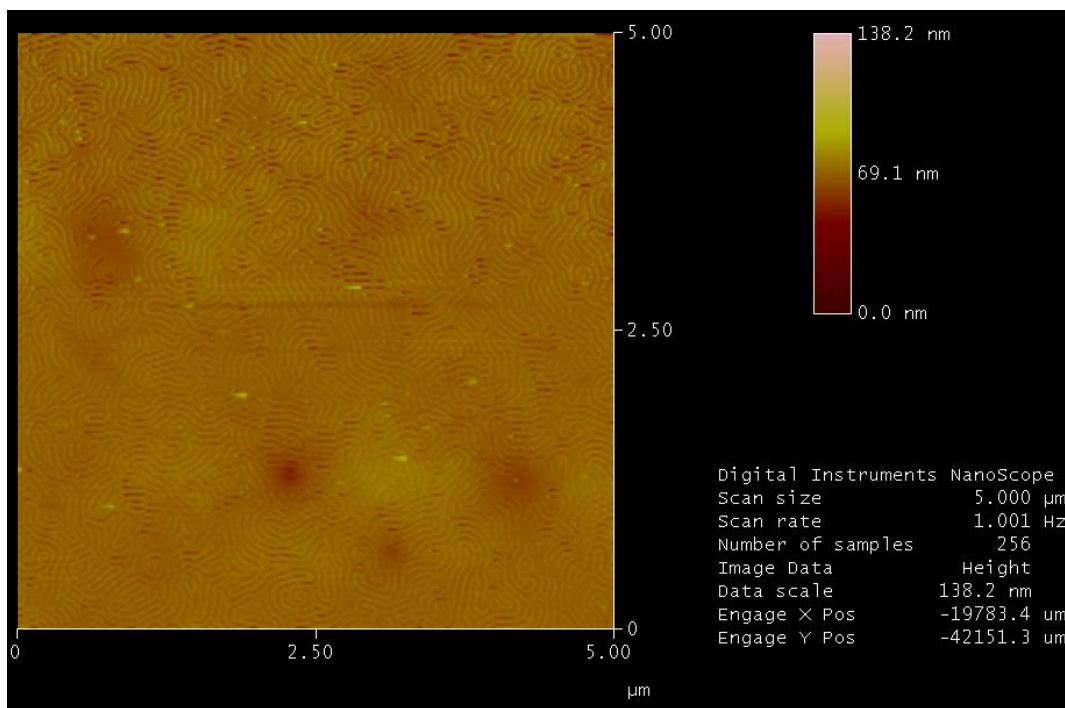


Figure 18: AFM image of the self assembled upright BCP lamellar structure on 3-MPTS treated silicon wafer with high coverage of 3MPTS.

5.1.3 Different Annealing Temperature For The Self Assembly Of BCP

Once satisfying results were obtained for coating of PS-b-PMMA on 3MPTS, we took the optimization process a little further and studied the effects of different annealing temperature on the formation of the lamellae micro-domains. The same procedure as the previous section was used to coat 3MPTS. The same process was also used to coat BCP on top of the 3MPTS, however, we kept the annealing time constant at 5 minutes and the annealing temperature was varied to 160 °C, 190 °C, 220 °C, and 250 °C. The process was followed by O₂ plasma etching to reveal the final BCP morphologies. Next, SEM and AFM images were taken to study the results. Figures 19 to 26 show the AFM and SEM images of these annealing temperatures.

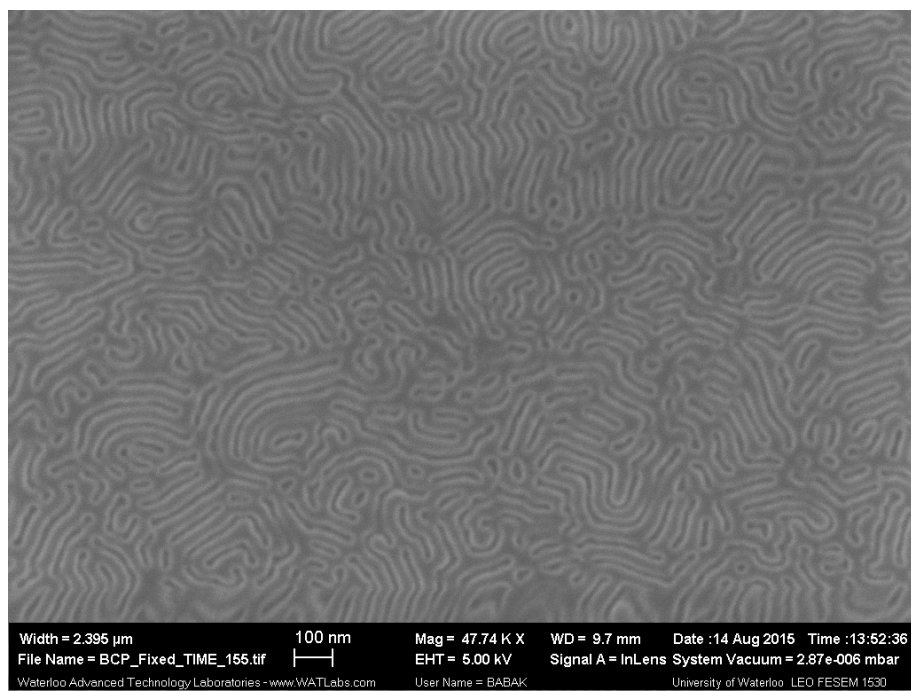


Figure 19: SEM image of the annealed BCP at 160°C for 5min.

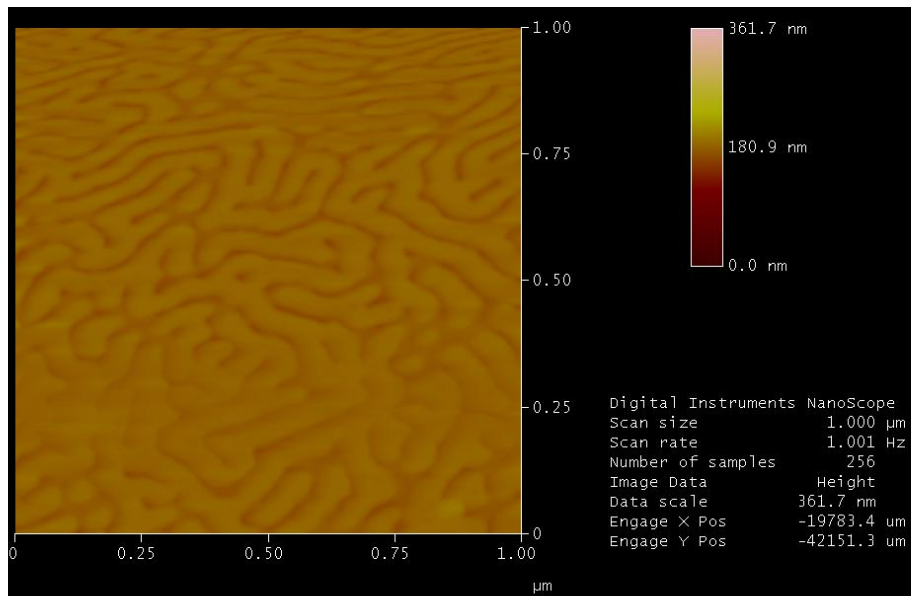


Figure 20: AFM image of the annealed BCP at 160°C for 5min.

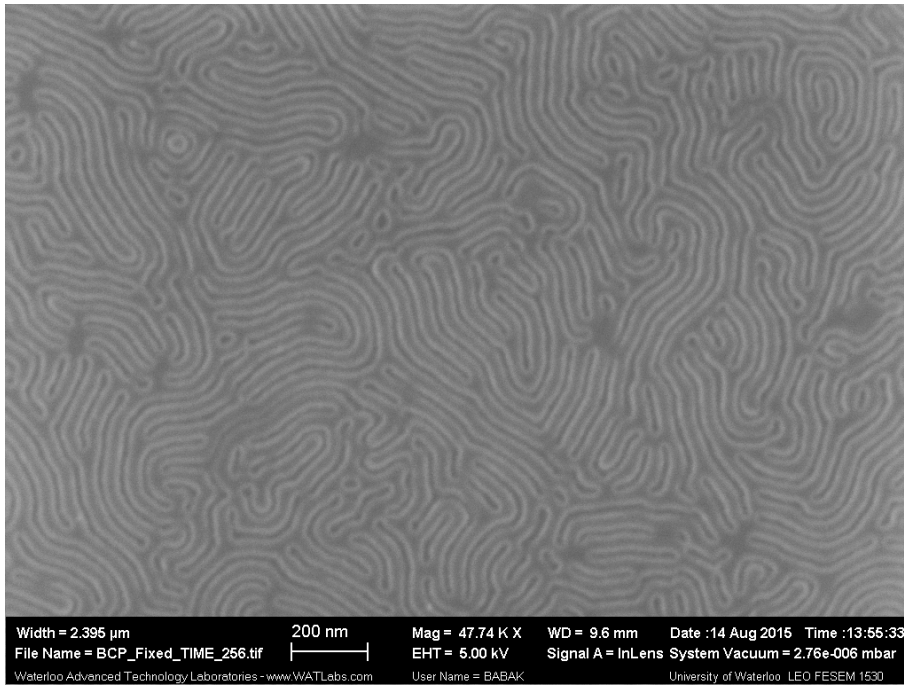


Figure 21: SEM image of the annealed BCP at 190°C for 5min.

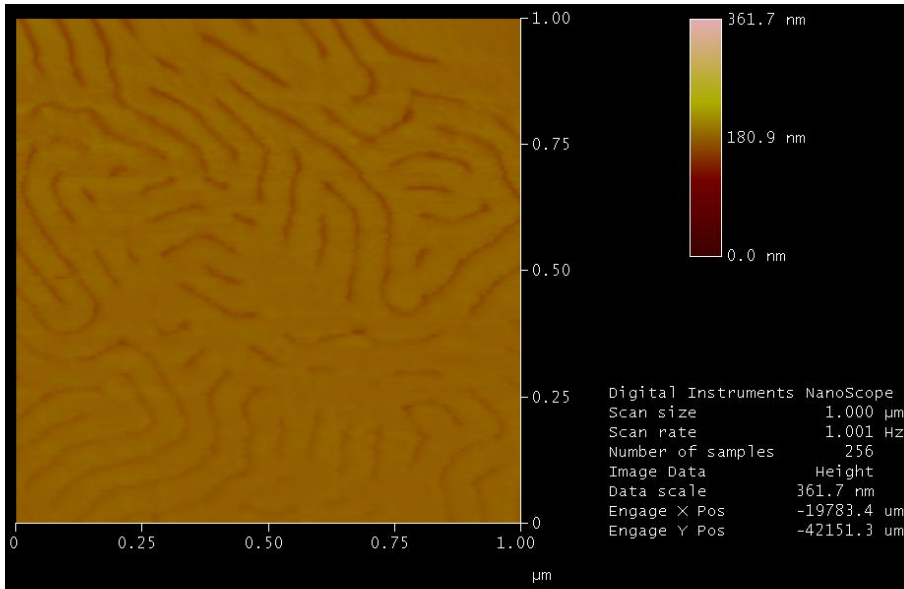


Figure 22: AFM image of the annealed BCP at 190°C for 5min.

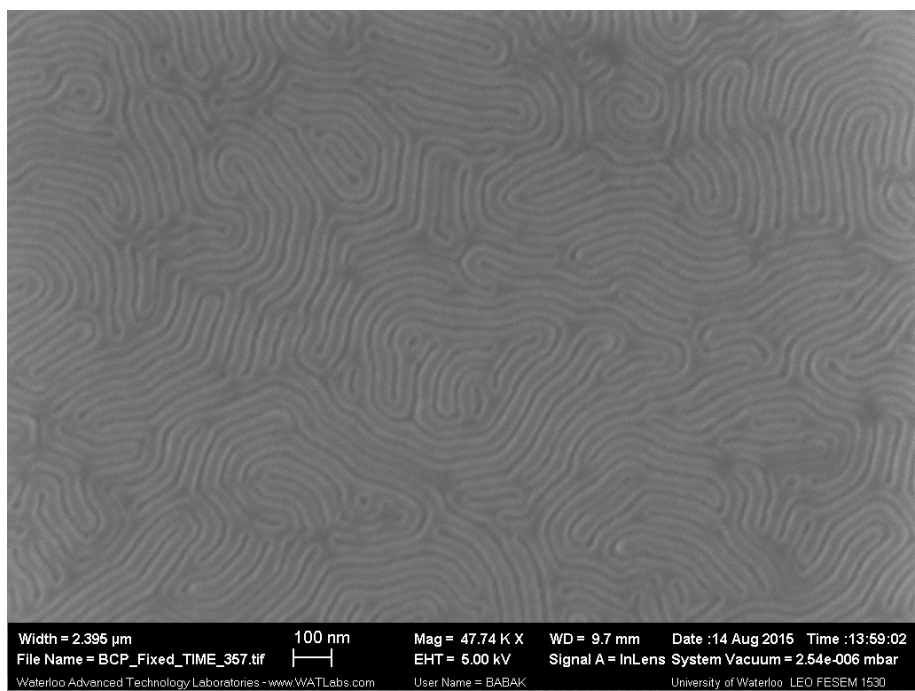


Figure 23: SEM image of the annealed BCP at 220°C for 5min.

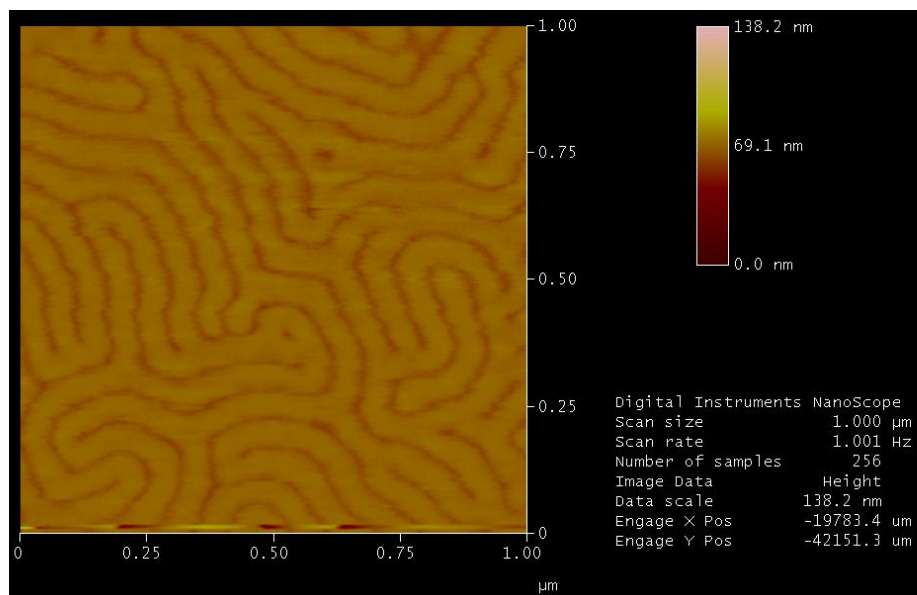


Figure 24: AFM image of the annealed BCP at 220°C for 5min.

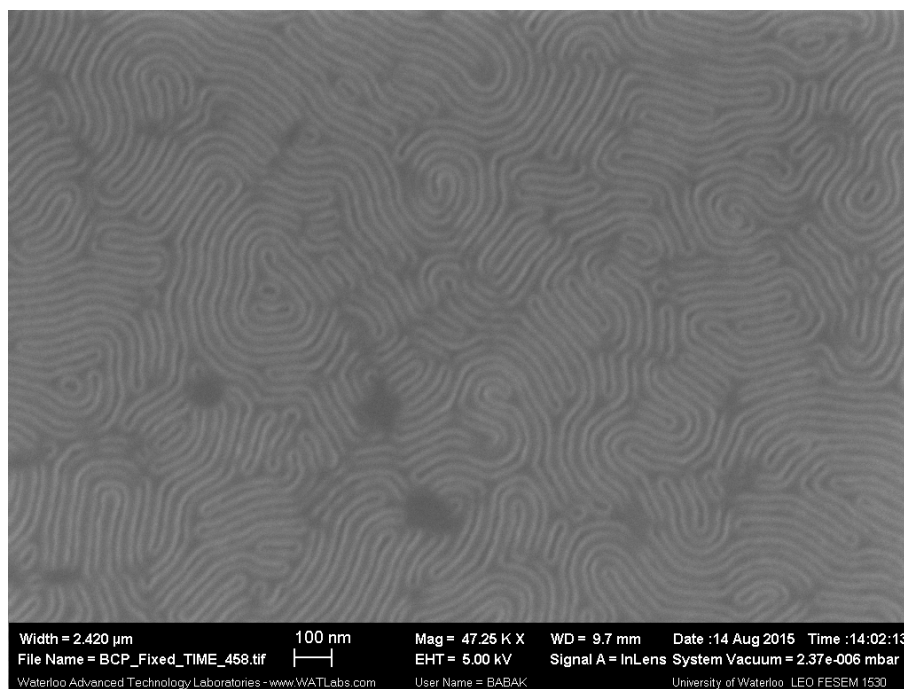


Figure 25: SEM image of the annealed BCP at 250°C for 5min.

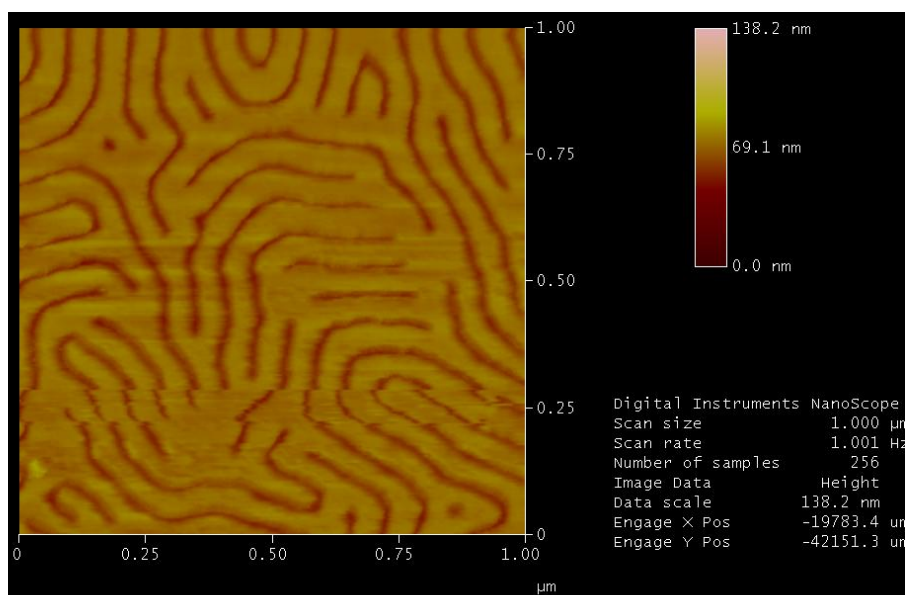


Figure 26: AFM image of the annealed BCP at 250°C for 5min.

5.1.4 Different Annealing Time For The Self Assembly Of BCP

After studying the effects of different annealing temperatures on morphologies of BCPs, we repeated the same procedure with varying times at 2 min, 6min, 20min, 60min, and a constant temperature of 190°C. All other steps were followed as in the previous section except the annealing time and temperature. SEM and AFM images were taken and are presented in figures 27 to 34.

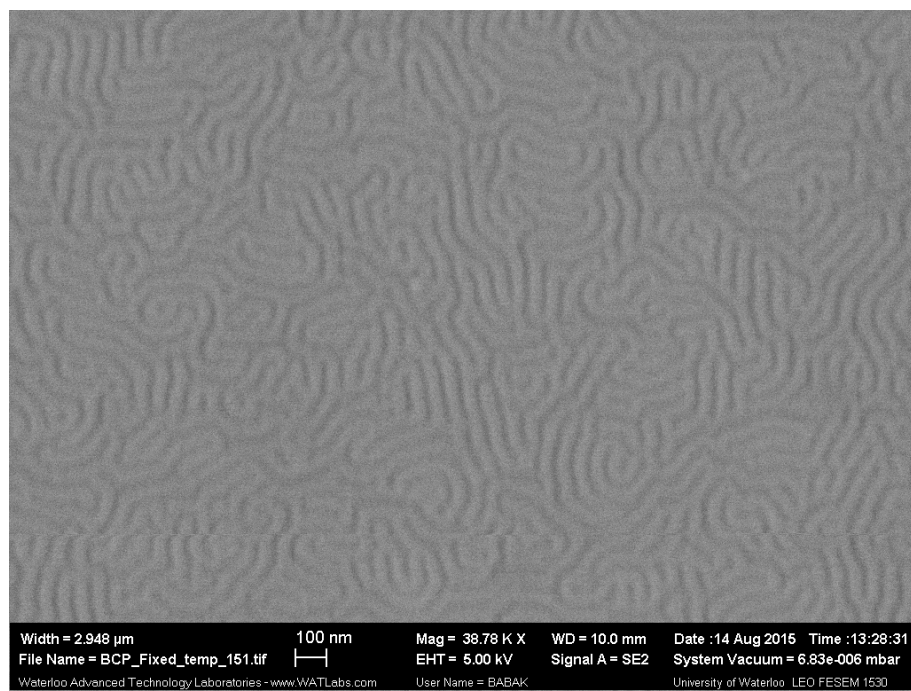


Figure 27: SEM image of the annealed BCP at 190°C for 2min.

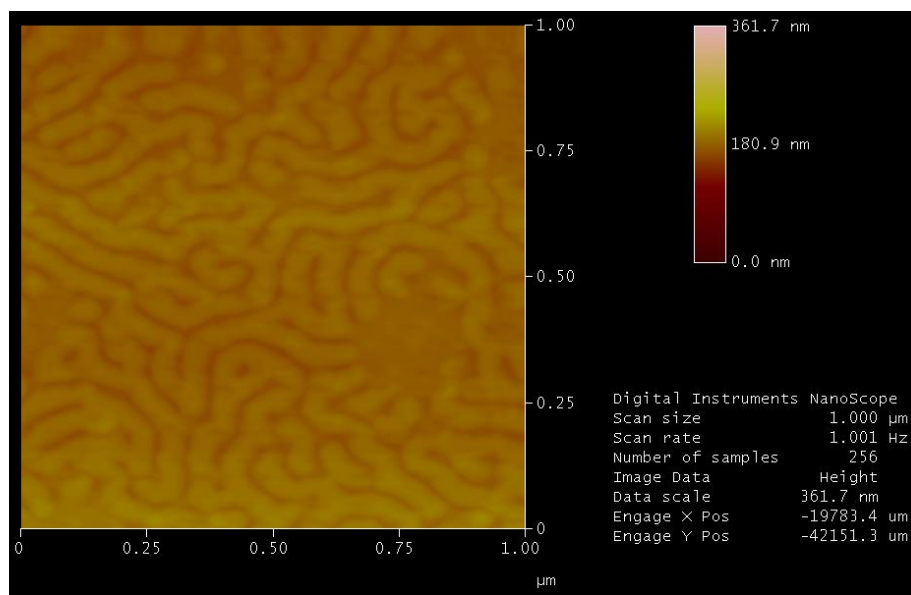


Figure 28: AFM image of the annealed BCP at 190°C for 2min.

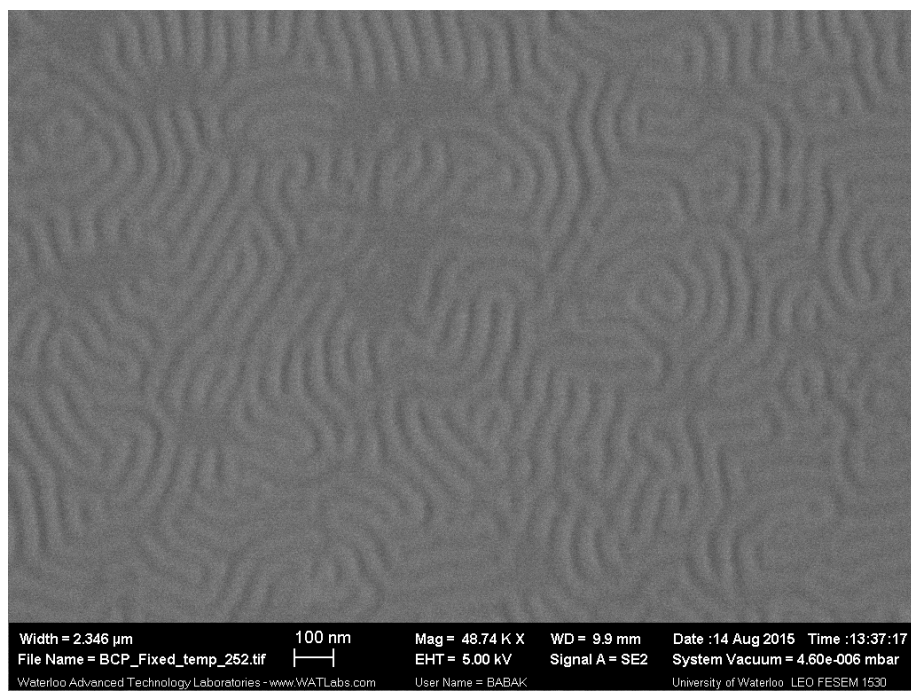


Figure 29: SEM image of the annealed BCP at 190°C for 6min.

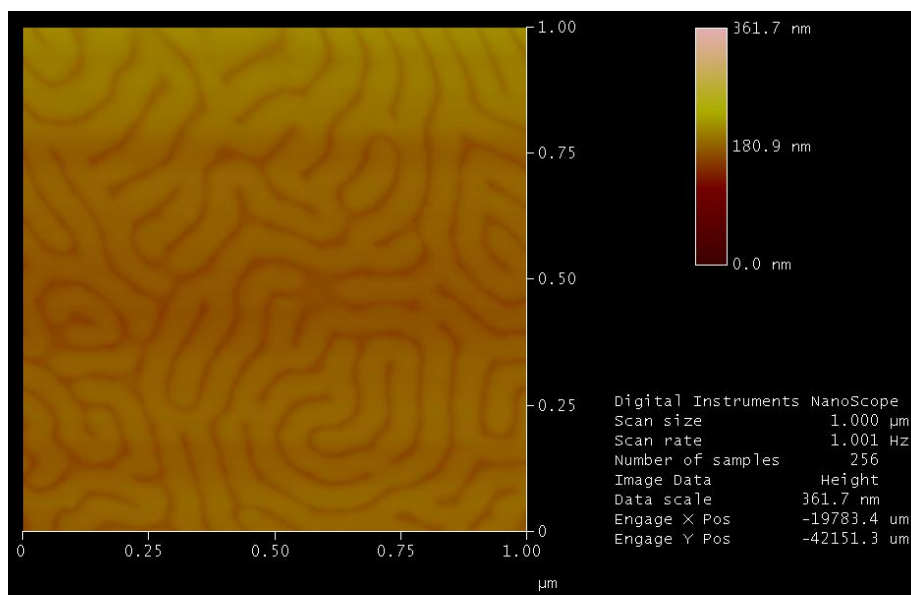


Figure 30: AFM image of the annealed BCP at 190°C for 6min.

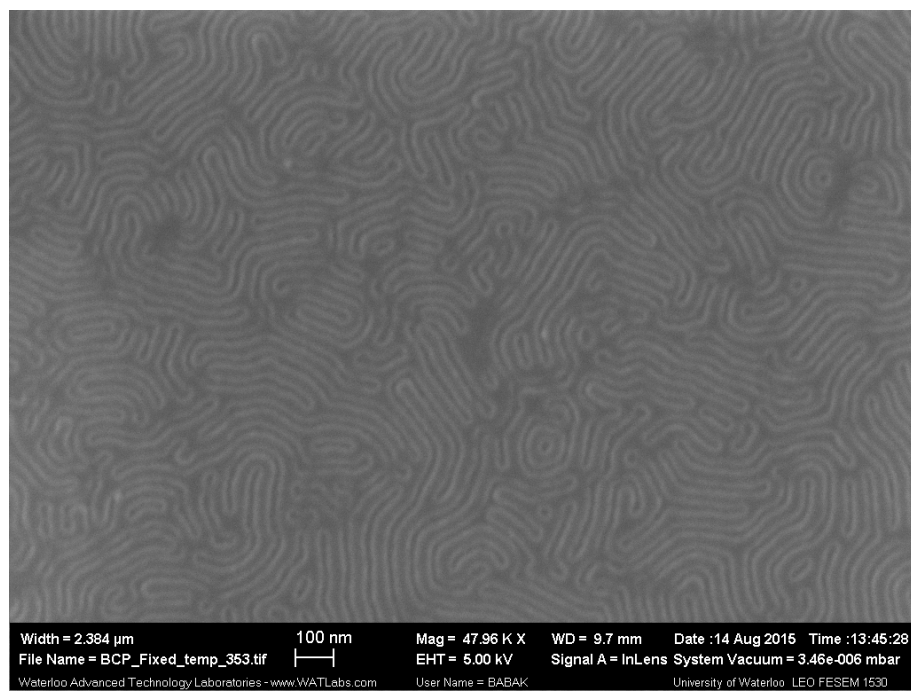


Figure 31: SEM image of the annealed BCP at 190°C for 20min.

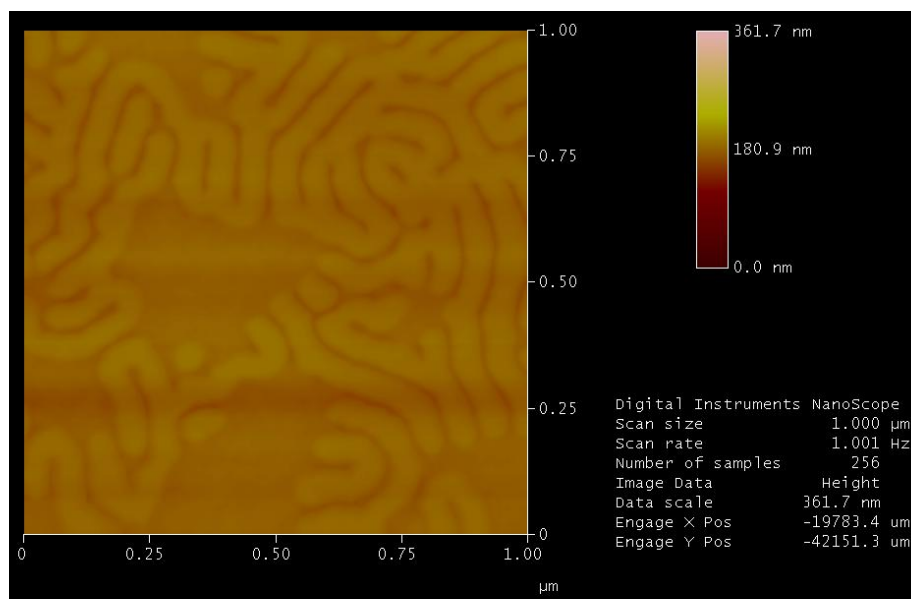


Figure 32: AFM image of the annealed BCP at 190°C for 20min.

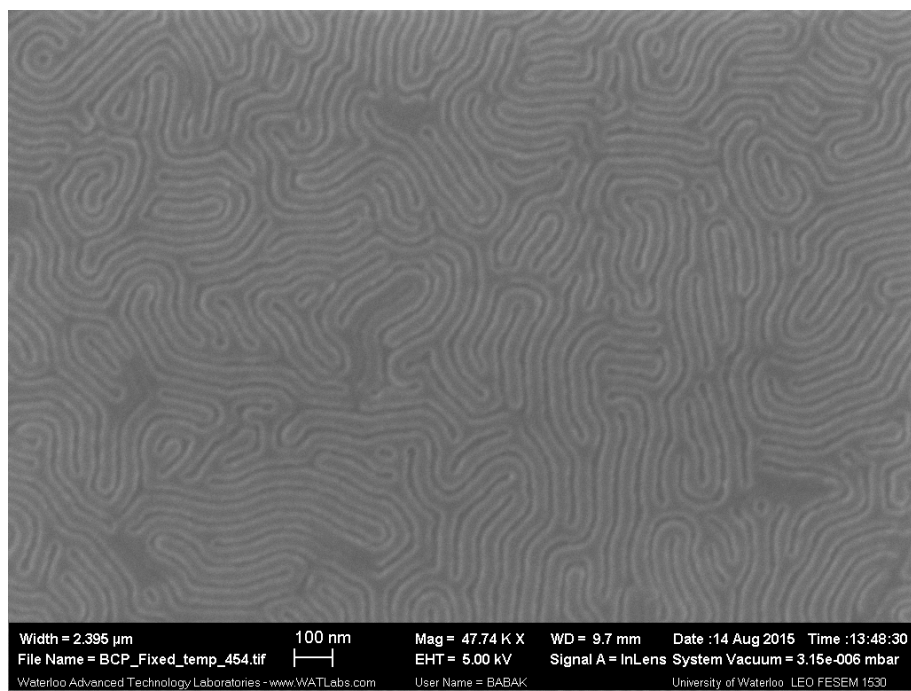


Figure 33: SEM image of the annealed BCP at 190°C for 60min.

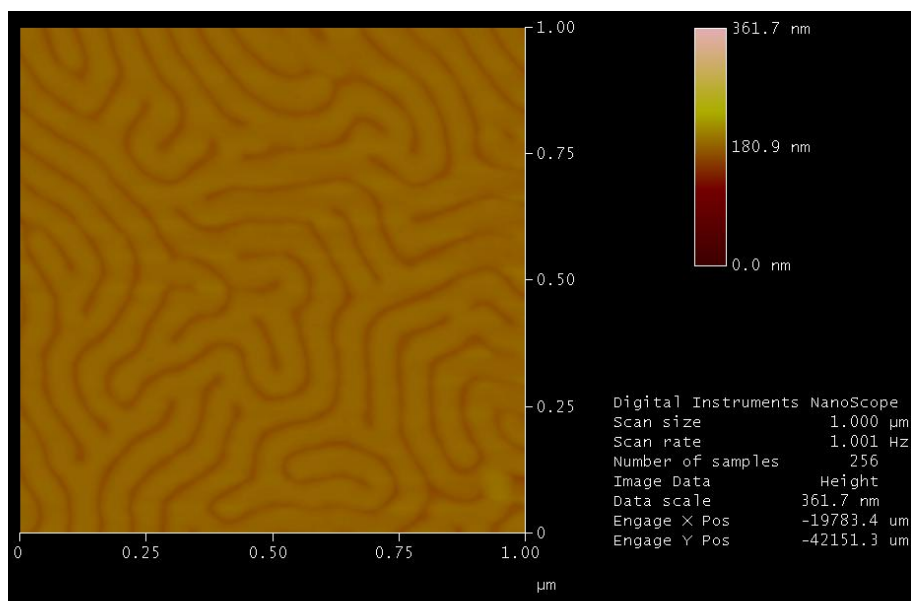


Figure 34: AFM image of the annealed BCP at 190°C for 60min.

5.1.5 Induced Morphologies On The Same BCP Thin Film By EBL

It is important to note that the centre-to-centre distance and the pore diameter in porous PS-*b*-PMMA templates can be controlled in several ways. One approach is to vary the molecular weight of the BCP. In this case, both the period and the diameter of the Lamellar microdomains will be varied together. In another approach, if the length of the PMMA block is varied either by adding more PMMA homopolymer to the BCP mix, or by cutting the chain shorter by breaking the PMMA chain. This modification can affect centre-to-centre distance by an amount that is commensurate with the length of the PMMA block. In this section we present the process by which PMMA blocks were selectively decomposed by the exposure to the electron beam. Areas that were exposed to the electron beam showed new induced morphologies. In this process, a clean (solvent and O₂ plasma cleaned) silicon wafer was treated with 3MPTS as was done in the previous section. PS-*b*-PMMA BCP was spin coated to get ~40nm thick film, the film was then baked at 90°C for 3mins. Next, the sample was exposed to e-beam at 5KeV, with I:118.7 pA, and a ranging dose of 5-40 $\mu\text{C}/\text{cm}^2$. Next, the exposed sample was developed in MIBK:IPA (1:3 ratio) for 1minute to removed the loos PMMA molecules, and was then annealed at 190°C for 20 minutes. In order to reveal the BCP patterns oxygen plasma (1 mtorr, 20 mW, 20 sccm, 10 sec) was performed. For a better visibility in the SEM and reduction of the charging effect during the SEM imaging, 10nm Chromium was deposited on top of the BCP film by the use of electron beam evaporation. Figure 32 shows the SEM image of the exposed BCP thin film with different dose for each square block ranging from 5 to 40 $\mu\text{C}/\text{cm}^2$. The patchy coverage of the BCP film is due to non-

uniform coverage of 3MPTS underlayer in this image.

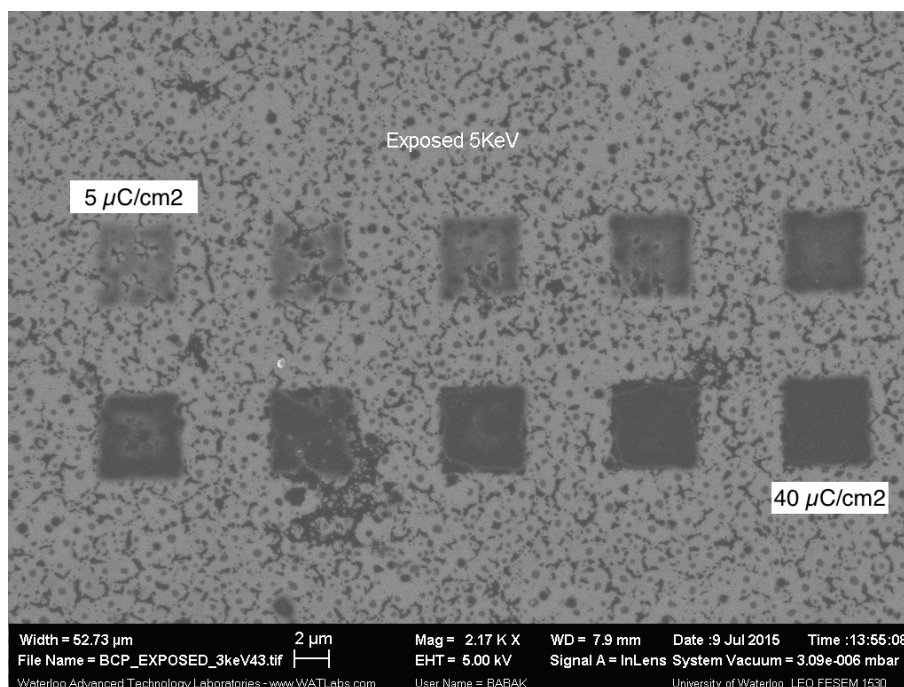


Figure 35: SEM image of the exposed BCP thin film by e-beam.

Selective zoomed-in SEM images of the exposed squares in figure 35 are presented next, this is to show the formation and the transition of the morphologies from lamellar to cylindrical in these areas. As it is evident from these images, when the exposure dose increases the morphology of the BCP changes. In Figure 36 the exposure dose is small so no significant damage is caused to the PMMA chain, however in figure 37 the dose is high enough to break the PMMA chains and create new morphology (close to cylindrical) in the exposed area. At very high exposure dose the surface energy could be modified so that preferential wetting of BCP blocks are more favored, hence promoting the lateral orientation of BCP. Another possibility is that at very high exposure dose, electron flux may damage the 3MPTS under-

layer and make it less resistive to the developer. These concepts may explain the appearance of the flat and smooth areas in figure 38.

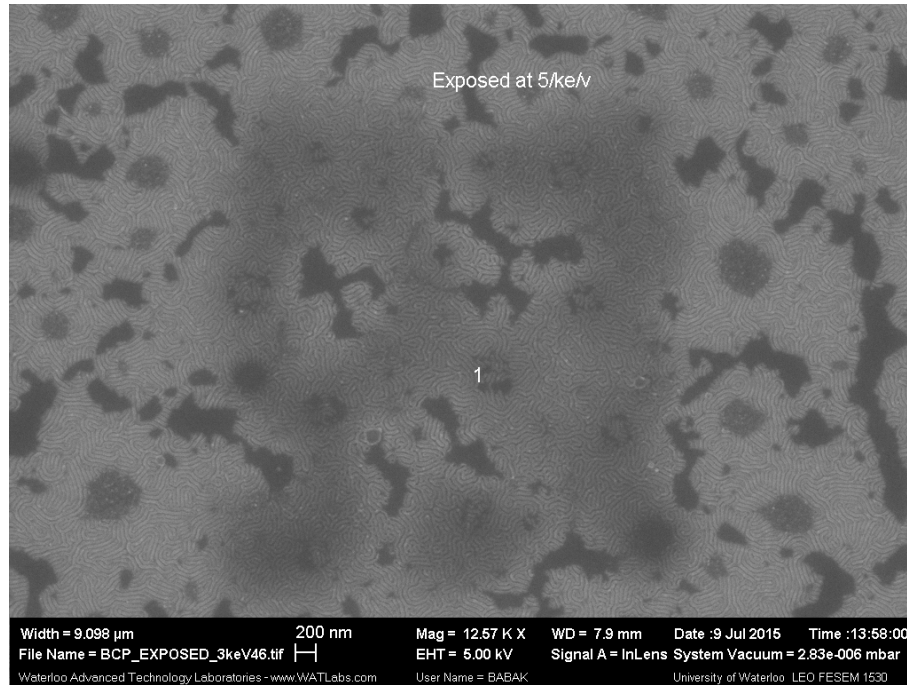


Figure 36: SEM image of the exposed BCP square at $5\mu\text{C}/\text{cm}^2$.

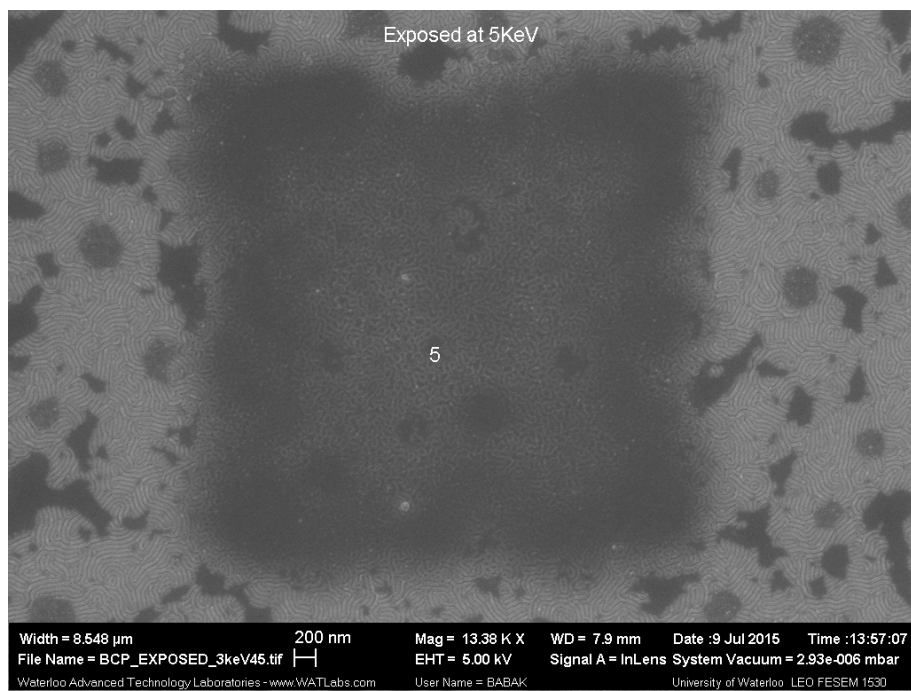


Figure 37: SEM image of the exposed BCP square at $12.60\mu\text{C}/\text{cm}^2$.

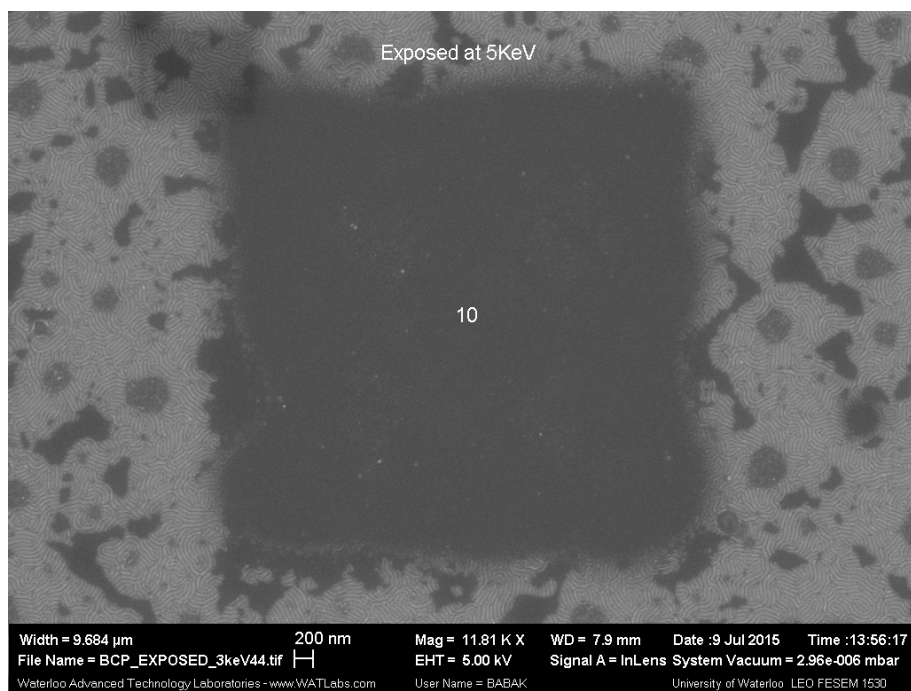


Figure 38: SEM image of the exposed BCP square at $40\mu\text{C}/\text{cm}^2$.

Chapter 6

6.1 Discussion

In this section an analysis for each process is presented in greater details.

6.1.1 Coating PS-b-PMMA BCP Thin Film

As it was shown in figures 12 and 13, BCP thin film of PS-b-PMMA did not form perpendicular lamellae structure. This was expected because non-treated silicon wafer has a native oxide which has higher affinity to wet the PMMA block in the the BCP. This preferential wetting of the BCP will lead to lateral stacking of the micro-domains within the thin film and hence, a flat and uniform film is formed. In figure 13, some finger print structures are visible, this formation could be possible due to different film thickness of the BCP in close proximity of the contaminates and artifacts. As we have discussed in section 3.1.4 film thickness could also change the orientation of the BCP. Therefore, in order to obtain perpendicular BCP morphologies surface treatment is a must.

6.1.2 Coating PS-b-PMMA BCP Thin Film With a Surface Neutralizing Underlayer

One of the most popular methods to obtain neutralize surface for the perpendicular self assembly of PS-b-PMMA block copolymer is to graft a random PMMA-r-PS copolymer brush with the same PS/PMMA ratio as the BCP. However, PMMA-r-PS with –OH terminated group is expensive and takes a long time to be grafted. Due to these limitations other alternatives are being studied. In section 3.1.4 we have summarized some of the most promising methods to

achieve perpendicular orientation for the lamellar structures and surface neutralization. In this report we make use of 3MPTS polymer which is neutral to both PS and PMMA blocks. B.H. Sohn and S. H. Yun first used SAM monolayer of 3MPTS to neutralize the interface, they coated the substrate by emerging the substrate into the solution of 3MPTS for 48 hours. Their coating process was very long which limits this method to lab testing and not for larger production purposes. In our experimental method we showed that evaporation of 3MPTS can be very effective since only a very small volume of 3MPTS is used, this process is very fast and can coat many substrates at a time if stacked together, this process is also free of contaminants compared to the liquid coating process. Both SEM and AFM imaging confirmed our hypothesis.

6.1.3 Different Annealing Temperature For The Self Assembly Of BCP

Different annealing temperatures were experimented in section 5.1.3, the main purpose was to decrease the annealing time required to form the perpendicular BCP structures. In doing so we found out that perpendicular structures can be formed in temperatures as low as 160°C and as high as 250°C. Both SEM and AFM images suggested that for temperatures of 220°C and 250°C the coherence length (how many fingerprint repeat units before it changes direction) of BCP is higher. Also, it was in our interest to find out whether high temperatures would affect the bonding of the films to each other or to the substrate. Polymer degradation and oxidization were among the other factors that were of the interest, however the images obtained for these studies confirmed that both monolayer and BCP layer stay attached to the interface, no sign of polymer degradation was visible in any of the images.

6.1.4 Different Annealing Time For The Self Assembly Of BCP

Similar to temperature studies, effect of varying time under constant annealing temperature was studied. The main purpose of this experiment was to reduce the annealing time for as much as possible to increase the throughput of the process. For the constant temperature of 190°C we learned that the annealing time can be reduced 2 minutes and still produce well defined perpendicular lamellar structures. Both SEM and AFM images confirm this finding.

6.1.5 Induced Morphologies On The Same BCP Thin Film By EBL

Lastly, e-beam lithography was used to modify the ratio of the PS-b-PMMA blocks locally and produce different morphologies within a same film. As it was mentioned before in this report, PMMA is a standard e-beam lithography resist. Exposure of the PMMA chains to electrons degrades the polymer and can reduce the polymer chain length. Degraded PMMA polymer can be removed by the developer. Annealing of the exposed BCP film allows the BCP blocks to move around and reach their stable energetic state, however since the PS and PMMA chains don't have equal chain lengths anymore, BCPs morphology will shift from lamellae to other morphologies according to the new ratio of the PS and PMMA blocks. In our experiment we were able to create two different morphologies by employing this technique. This effect clearly is visible in figures 40, which is a blown up section of the exposed square of the PS-b-PMMA with 5KeV and the exposure dose of $12.60\mu\text{C}/\text{cm}^2$.

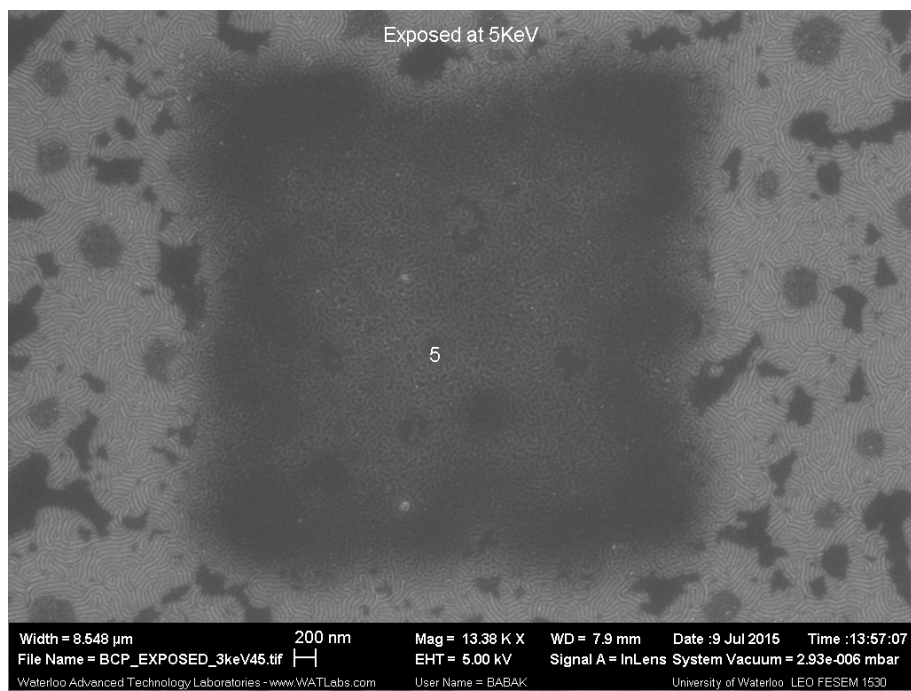


Figure 39: SEM image of exposed PS-b-PMMA BCP by e-beam.

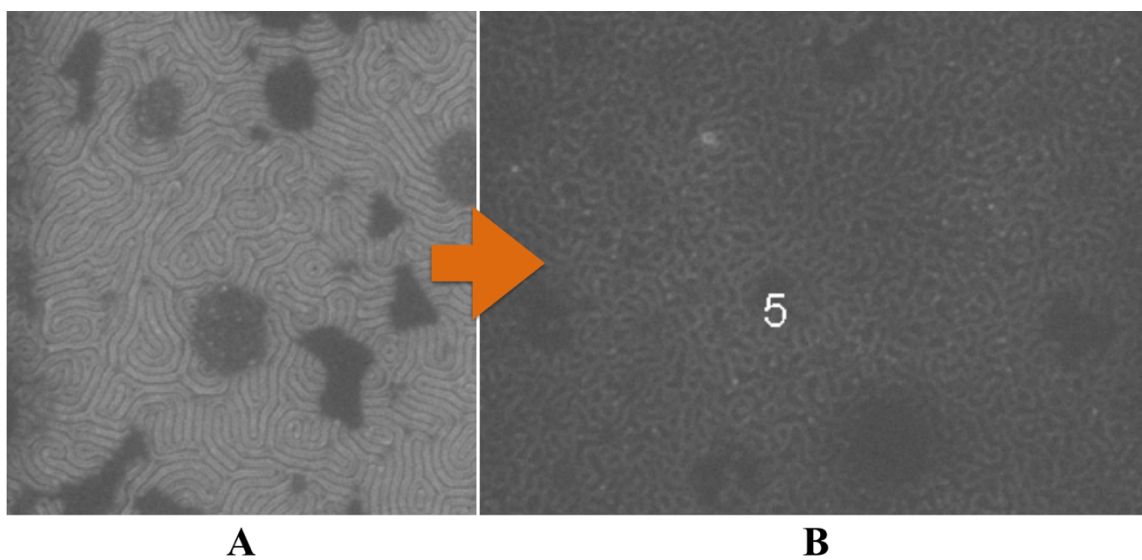


Figure 40: SEM image of exposed PS-b-PMMA BCP by e-beam. a) Non-exposed area which shows the well defined finger print patterns. b) Exposed area by e-beam which shows morphologies other than finger print.

References

- [1] ITRS, “International technology roadmap for semiconductors,” 2011. [Online]. Available: <http://www.itrs.net>.
- [2] S. Park, D. H. Lee, J. Xu, B. Kim, S. W. Hong, U. Jeong, T. Xu, and T. P. Russell, “Macroscopic 10-terabit-per-square-inch arrays from block copolymers with lateral order.,” *Science*, vol. 323, no. 5917, pp. 1030–1033, 2009.
- [3] M. Luo and T. H. Epps, “Directed block copolymer thin film self-assembly: Emerging trends in nanopattern fabrication,” *Macromolecules*, vol. 46, no. 19, pp. 7567–7579, 2013.
- [4] K. Galatsis, K. L. Wang, M. Ozkan, C. S. Ozkan, Y. Huang, J. P. Chang, H. G. Monbouquette, Y. Chen, P. Nealey, and Y. Botros, “Patterning and templating for nanoelectronics,” *Adv. Mater.*, vol. 22, no. 6, pp. 769–778, 2010.
- [5] I. Bitá, J. K. W. Yang, Y. S. Jung, C. A. Ross, E. L. Thomas, and K. K. Berggren, “Graphoepitaxy of self-assembled block copolymers on two-dimensional periodic patterned templates.,” *Science*, vol. 321, no. 5891, pp. 939–943, 2008.
- [6] V. Mishra, G. H. Fredrickson, and E. J. Kramer, “Effect of film thickness and domain spacing on defect densities in directed self-assembly of cylindrical morphology block copolymers,” *ACS Nano*, vol. 6, no. 3, pp. 2629–2641, 2012.
- [7] B. Sohn, “Perpendicular lamellae induced at the interface of neutral self-assembled monolayers in thin diblock copolymer films,” *Polymer (Guildf.)*, vol. 43, no. 8, pp. 2507–2512, 2002.
- [8] L. C. by Geoffrey A Ozin, André Arsenault, *Nanochemistry: A Chemical Approach to Nanomaterials*. 2008.
- [9] X. Gu, I. Gunkel, T. P. Russell, and T. P. Russell, “Pattern transfer using block copolymers Subject Areas : Author for correspondence :,” 2013.
- [10] F. S. Bates and G. H. Fredrickson, “Block copolymer thermodynamics: theory and experiment.,” *Annu. Rev. Phys. Chem.*, vol. 41, pp. 525–557, 1990.
- [11] H. C. Kim, S. M. Park, W. D. Hinsberg, and I. R. Division, “Block copolymer based nanostructures: Materials, processes, and applications to electronics,” *Chem. Rev.*, vol. 110, no. 1, pp. 146–177, 2010.

- [12] S. B. Darling, "Directing the self-assembly of block copolymers," *Prog. Polym. Sci.*, vol. 32, no. 10, pp. 1152–1204, 2007.
- [13] X. Gu, I. Gunkel, T. P. Russell, and T. P. Russell, "Pattern transfer using block copolymers" 2013.
- [14] C. Park, J. Yoon, and E. L. Thomas, "Enabling nanotechnology with self assembled block copolymer patterns," *Polymer (Guildf)*, vol. 44, no. 22, pp. 6725–6760, 2003.
- [15] A. P. Marencic and R. a. Register, "Controlling Order in Block Copolymer Thin Films for Nanopatterning Applications," *Annu. Rev. Chem. Biomol. Eng.*, vol. 1, no. 1, pp. 277–297, 2010.
- [16] P. Mansky, T. Russell, C. Hawker, J. Mays, D. Cook, and S. Satija, "Interfacial Segregation in Disordered Block Copolymers: Effect of Tunable Surface Potentials," *Physical Review Letters*, vol. 79, no. 2. pp. 237–240, 1997.
- [17] P. Mansky, T. P. Russell, C. J. Hawker, M. Pitsikalis, and J. Mays, "Ordered diblock copolymer films on random copolymer brushes," *Macromolecules*, vol. 30, no. 22, pp. 6810–6813, 1997.
- [18] E. Han, K. O. Stuen, Y. H. La, P. F. Nealey, and P. Gopalan, "Effect of composition of substrate-modifying random copolymers on the orientation of symmetric and asymmetric diblock copolymer domains," *Macromolecules*, vol. 41, no. 23, pp. 9090–9097, 2008.
- [19] R. D. Peters, X. M. Yang, T. K. Kim, B. H. Sohn, and P. F. Nealey, "Using self-assembled monolayers exposed to X-rays to control the wetting behavior of thin films of diblock copolymers," *Langmuir*, vol. 16, no. 10, pp. 4625–4631, 2000.
- [20] S. O. Kim, H. H. Solak, M. P. Stoykovich, N. J. Ferrier, J. J. De Pablo, and P. F. Nealey, "Epitaxial self-assembly of block copolymers on lithographically defined nanopatterned substrates.," *Nature*, vol. 424, no. 6947, pp. 411–414, 2003.
- [21] E. Sivaniah, Y. Hayashi, S. Matsubara, S. Kiyono, T. Hashimoto, K. Fukunaga, E. J. Kramer, and T. Mates, "Symmetric diblock copolymer thin films on rough substrates. Kinetics and structure formation in pure block copolymer thin films," *Macromolecules*, vol. 38, no. 5, pp. 1837–1849, 2005.
- [22] L. Y. B. A, J. He, K. Sill, and H. Xiang, "Self-directed self-assembly of nanoparticle / copolymer mixtures," *Nature*, vol. 404, pp. 55–59, 2005.

- [23] Park SC, Kim BJ, Hawker CJ, Kramer EJ, Bang J, Ha JS, “Controlled ordering of block copolymer thin films by the addition of hydrophilic nanoparticles,” *Macromolecules* 40:8119–24, 2007.
- [24] U. Jeong, D. Y. Ryu, D. H. Kho, J. K. Kim, J. T. Goldbach, D. H. Kim, and T. P. Russell, “Enhancement in the Orientation of the Microdomain in Block Copolymer Thin Films upon the Addition of Homopolymer,” *Adv. Mater.*, vol. 16, no. 6, pp. 533–536, 2004.
- [25] J. Y. Wang, W. Chen, J. D. Sievert, and T. P. Russell, “Lamellae orientation in block copolymer films with ionic complexes,” *Langmuir*, vol. 24, no. 7, pp. 3545–3550, 2008.
- [26] T. Thurn-Albrecht, J. Derouchey, T. P. Russell, and H. M. Jaeger, “Overcoming interfacial interactions with electric fields,” *Macromolecules*, vol. 33, no. 9, pp. 3250–3253, 2000.
- [27] T. Xu, Y. Zhu, S. P. Gido, and T. P. Russell, “Electric Field Alignment of Symmetric Diblock Copolymer Thin Films,” *Macromolecules*, vol. 37, no. 7, pp. 2625–2629, 2004.
- [28] R. a. Segalman, “Patterning with block copolymer thin films,” *Mater. Sci. Eng. R Reports*, vol. 48, no. 6, pp. 191–226, 2005.
- [30] R. J. Albalak and E. L. Thomas, “Microphase separation of block copolymer solutions in a flow field,” *J. Polym. Sci. Part B Polym. Phys.*, vol. 31, no. 1, pp. 37–46, 1993.
- [31] M. Kimura, M. J. Misner, T. Xu, S. H. Kim, and T. P. Russell, “Long-range ordering of diblock copolymers induced by droplet pinning,” *Langmuir*, vol. 19, no. 23, pp. 9910–9913, 2003.
- [32] Y.-R. Hong, D. H. Adamson, P. M. Chaikin, and R. A. Register, “Shear-induced sphere-to-cylinder transition in diblock copolymer thin films,” *Soft Matter*, vol. 5, no. 8, p. 1687, 2009.
- [33] B. C. Berry, A. W. Bosse, J. F. Douglas, R. L. Jones, and A. Karim, “Orientational order in block copolymer films zone annealed below the order-disorder transition temperature,” *Nano Lett.*, vol. 7, no. 9, pp. 2789–2794, 2007.
- [34] L. Oria, A. Ruiz De Luzuriaga, J. A. Alduncin, and F. Perez-Murano, “Polystyrene as a brush layer for directed self-assembly of block co-polymers,” *Microelectron. Eng.*, vol. 110, pp. 234–240, 2013.

- [35] “RAITH150-TWO product info,” 2014. [Online]. Available: http://www.nmf.ncsu.edu/sites/default/files/RAITH150-TWO_product_info.pdf.
- [36] M. A. Mohammad, M. Muhammad, S. K. Dew, and M. Stepanova, “Fundamentals of Electron Beam Exposure and Development,” in *Nanofabrication: Techniques and Principles*, 2012, p. 344.